Hindawi
Advances in Civil Engineering
Volume 2022, Article ID 6934078, 30 pages
https://doi.org/10.1155/2022/6934078

Review Article

Structures under Synergetic Effects of Combined Blast and Impact Loads: A State-of-the-Art Review

Solomon Abebe [1] **and Tesfaye Alemu Mohammed** [2,3]

[1]*Civil Engineering Department, Debre Markos University, Debre Marqos, Ethiopia*
[2]*Civil Engineering Department, Addis Ababa Science and Technology University, Addis Ababa, Ethiopia*
[3]*Construction Quality and Technology Center of Excellence, Addis Ababa Science and Technology University, Addis Ababa, Ethiopia*

Correspondence should be addressed to Tesfaye Alemu Mohammed; tes.alemu@gmail.com

Received 15 February 2022; Revised 16 April 2022; Accepted 28 April 2022; Published 2 July 2022

Academic Editor: Roberto Nascimbene

Copyright © 2022 Solomon Abebe and Tesfaye Alemu Mohammed. This is an open access article distributed under the Creative Commons Attribution License, which permits unrestricted use, distribution, and reproduction in any medium, provided the original work is properly cited.

When the effect of combined blast induced shock wave and fragment penetration impact load is sufficiently large enough to induce severe damage in structures compared to individual actions of only-blast and only-impact load, this scenario is called synergetic effect of simultaneous actions. The combined nature of those dual actions aggravates damage and collapses of structures. This paper presented the state-of-the-art review on effect of different parameters, dynamic responses, failure types, and damage mitigation techniques for structures prone to combined actions of blast induced shock wave and fragment impact loads based on findings of experimental, numerical, and analytical research works conducted in previous literature.

1. Introduction

Accidental loads such as blast and impact loads are most extreme load cases on which their probability of occurrence is very low, but once they occurred, they have a devastating damage on a given structure. It is obvious that no civilian buildings can be designed to bear all types of damage resulting from accidental actions such as blast and impact loads. But, the need for studying complicated nature of accidental loads specifically combined effects of blast-impact loads is very crucial and nowadays engineers give due consideration on synergetic effects of combined blast and impact loads in analysis and design phases of very important buildings and infrastructures.

When an explosive material is initiated to detonate, part of the energy (1/3) converted as a blast induced shock wave which travels to a surrounding air in radial form, and the remaining energy (2/3) imposes an imparted pressure to fragmenting the case, on which these fragments travel to a surrounding air as a striking body DOD [1]. This scenario makes a combined effects of blast and impact loads, typically the blast-impact load on which the blast induced shock wave hits a structure prior to a striking body [2, 3]. Researchers anticipated that synergetic effects of combined blast-impact (or impact-blast) loading scenario could happen in another different conditions. One example is a cased explosive material with large scaled distances detonates on which the fragments from the case hit a given structure prior to blast induced shock wave; another example is the case on which vehicles and vessels carrying explosive materials crashed with a barrier (structure) leading a first impact load followed by explosion from the cargo points which may also be combined loading cases of impact-blast [4, 5].

Due to the reason of risks, expensiveness, and security reasons, currently there are very limited experimental studies in the literature for the combined loading effects of blast and impact, when compared to numerical studies. Few authors [6–12] explicitly investigated synergetic effects of combined blast and impact loads on reinforced concrete beams and columns. Similarly, researches on dynamic effects of combined blast-impact load on RC slabs were conducted by [13–15]. Moreover the papers [3, 16–18] numerically

studied combined effects of blast and fragment loading on walls whereas researchers [19–25] investigated combined blast-impact loading scenario on different plates, panels, and decks. Furthermore, combined effect of aforementioned loading scenario was also investigated on mass concrete [4, 26, 27].

1.1. Technical Design Manuals. Currently, synergetic combined effects of blast and impact loads are not considered in major design codes and engineers are not as well practicing application of simultaneous load cases during structural design phases. ASCE [28] listed lack of general awareness, unexpected, and unexplored nature of accidental loads as main factors for the reason why such simultaneous actions of accidental loads are not considered in practice. Despite limiting factors, there are some design guidelines and standards prepared for structures under accidental loads (see Table 1).

A few manuals [1, 29–32] presented guidelines for analysis, design, and damage mitigation techniques for structures under explosion effects. CSA [30] explicitly discussed acceptance criteria and regulations for structural integrity and mitigation of disproportionate collapse of frame systems against blast load whereas manuals [1, 29, 31, 32] provided typical detailing schemes for concrete, steel, and composite structures.

Among available guidelines, DOD [1] presented a brief introduction on blast, fragment, and shock loads in both confined and unconfined explosion cases. In contrary to other guidelines, DOD [1] has charts for both spherical and hemispherical TNT explosion scenarios. Those charts are sometimes called Spaghetti curves and are always critical parameters to be considered for analysis and design of blast resistant structures.

Besides this, all design manual guidelines share a commentary point on material properties under high strain rate; structural analysis and design; and assessment and mitigation techniques for concrete, steel, composite, and masonry structures against explosion related effects.

Guidelines [33, 34] synthesized an impact induced load from vessel collision and simplifies impact loading case by an equivalent static load based on deformation-force and kinetic energy of the impactor (vessels). On the other hand, UK's highway agency [35] forwarded a suggestion on effect of vehicle collision based on experimentally reported equivalent nominal loads applied horizontally on bridge columns.

1.2. Theoretical Background. Explosion is a sudden release of energy which is possible by extreme ignition of highly combustion material which makes expansion of gases in rapid mode. This expansion of gases makes a transient change in atmospheric air and radially moves from the source of explosion to point of interest at supersonic speed making a shock front in; this shock front pressure is blast wave [1, 2, 29, 30, 37]. On the other hand, impact load is one type of impulsive load which results from collision of two bodies, one with an initial speed hitting another being at rest. Impulsive loading induced loading can result in strain rates in ranges of $10^{\circ}s^{-1}$ to $10^{2}\ s^{-1}$ whereas blast loads typically produce very high strain rate of $10^{2}\ s^{-1}$ to $10^{4}\ s^{-1}$ (Figure 1) [38].

There are two types of blast waves, namely, shock wave and pressure wave [29]. The former one (shock wave) is characterized by its capacity to suddenly change ambient atmospheric pressure to a peak overpressure. After spending a specified positive time duration, this peak overpressure then returns to ambient pressure. Also, it even drops beyond ambient pressure revealing a suction effect. As opposed to shock wave, pressure wave has a gradual pressure rise to peak overpressure followed by a respective drop in pressure to negative phase (Figure 2).

On the other hand, there are two types of impact loads, namely, soft and hard impact [37]. Soft impact is characterized by the case when kinetic energy of a striking body is completely transferred into deformation energy of a striking energy, while rigidly assumed body at rest remains intact and undeformed (Figure 3(a)). Explosive load resulting in a blast induced shock wave is usually not influenced by a structure's deformation and belongs to soft impact category, whereas hard impact occurs when a striking body is rigid on which kinetic energy of a striker is much largely absorbed by deformation of a struck body (Figure 3(b)).

2. Methods of Analysis

Available methods for analysis of structures subjected to combined blast-impact loads can be classified into four themes:

(i) Analytical methods
(ii) Empirical methods
(iii) Experimental methods
(iv) Numerical methods

Analytical methods are typically based on general continuum mechanics equations (i.e., law of conservation of energy and momentum) in which kinematics and mechanical response of materials are modeled as a continuous mass, not as discrete entities. Manuals [29, 30] listed some methods that can be used for analysis of structures under accidental loads including single-degree-of-freedom (SDOF) and multi-degree-of-freedom (MDOF); both methods represent displacement in single coordinates. SDOF can be used based upon some simplifications including single equivalent mass, stiffness, and damping parameters in a model whereas MDOF is another refined method, on which a given structure is simplified by series of lumped masses, stiffnesses, and damping parameters. Despite simplification and ease preliminary rough estimations, analytical methods have shortcomings such as incapability to represent and capture complex boundaries, loadings, and local failures or damage modes.

Empirical methods are mainly correlations with experimentally reported data. But this approach is limited to the extent of referenced experimental parameters. Experimental study (both field and/or laboratory) is based on controlled

Table 1: Design code of practices for structures subjected to blast and impact loads.

Year	Code/guideline	Remark
2012	Design and assessment of buildings under to blast loads, CSA	Structural design envelope and mitigation technical provisions CSA [30]
2010	Design of blast resistant buildings in petrochemical facilities; 2nd ed, ASCE	Introduce load determination systems, type of analysis, method construction, and detailing of connections ASCE [29]
2009	Guide specification and commentary for vessel collision design and highway bridges, AASHTO	Applicable for vehicle collision. Use equivalent static load based on performance-force method of analysis AASHTO [33]
2008	Unified facilities criteria (UFC), prepared by dep. of the army, navy, air force	Brief explanation on blast, fragment, and shock loads. Introduce methods of analyses, and structural designs DOD [1]
2004	The design of highway bridges for vehicle collision loads, prepared by department of transport, UK	Applicable for vehicle collision and bases equivalent nominal loads applied horizontally UK's-Highway-Agency [35]
2003	Actions on structures. European committee (CEN)	Use equivalent static force with effect of different parameters CEN [34]
2003	Federal emergency management agency (FEMA), prepared by department of homeland security	Forward threat, vulnerability, and risks on structures. Introduce methods of site layout and design guidance FEMA [36]
2003	Minimum design loads for buildings and other structures (ASCE 7–98)	Introduce on how additional loads such as vibration and impact loads can be induced in structural design phases ASCE [28]
1986	Blast resistant structures: design manual 2.08., NAFEC	Introduce blast types, structural design for blast load NAFEC [31]
1980	A manual for prediction of blast and fragment loadings, DOE	Methods for predict different blast loading, cratering, ground shock, and fragmentation DOE [32]

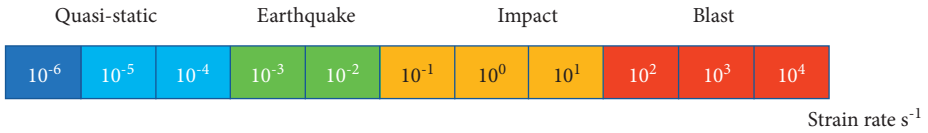

Figure 1: Range of strain rate for different type dynamic loading.

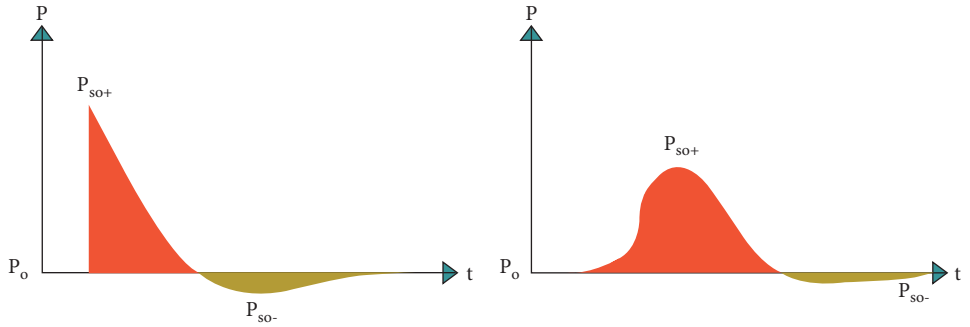

Figure 2: Characteristic shapes of blast waves: (a) shock and (b) pressure waves.

Figure 3: Impact types: (a) soft impact and (b) hard impact.

environment and parameters with a given well-known specimen under consideration. Moreover, the numerical method (or sometimes known as first-principle) based on mathematical and constitutive equations which describes basics laws of physics governing a problem under conservation of mass, energy, and momentum.

In the domain of civil engineering structures, especially for structures susceptible to accidental loads including blast and impact loads, analytical use of analysis may provide a suitable platform to get global effects of structures; however, this does not capture local effects and damage. Furthermore, use of experimental methods for explosion related studies makes it expensive and risky. On the other hand, while good engineering judgment is employed in the accuracy, mesh sensitivity, material model selection criteria, and use of numerical method provide good precisions with less risk, duration, computational cost, iterations, and cycles. Currently, many commercial finite element computer programs including ABAQUS, ANSYS, DYNA 3D, LS-DYNA, ADINA, MSC NASTRAN, and NASTRAN are available for simulation of explosions and related effects ASCE [29].

3. Material Properties

3.1. Material Modelling. Mechanical properties of any engineering materials are characterized by stress-strain relationship elucidated in

$$\sigma = f(\varepsilon), \tag{1}$$

and taking strain rate and load history into account equation (1) leads to

$$\sigma = f(\varepsilon, \dot{\varepsilon}, \varsigma). \tag{2}$$

From equation (2), it is noted that different material models are needed to capture real behavior of various materials and respective loading conditions. Due to these reasons, computational FEA programs such as ABAQUS, ANSYS, DYNA, LS-DYNA, ADINA, MSC NASTRAN, and NASTRAN account different theories and applications of material modelling techniques [39].

Material models based on linearity of elastic models can be classified as linear and nonlinear materials models. Linear elastic models are known by their simplicity on which a strain that caused a given stress is directly proportional and have a linear type of relation. Obviously, it is not suitable for accidental dynamic loads, whereas nonlinear material model accounts for a relation beyond linear elastic proportionality limits of a material.

Based on viscoelasticity perspectives, material models can be clustered as viscoelastic and plastic models. Viscoelastic models are known for their inclusiveness of creep and relaxation cases, whereas viscoplastic models are best well known for description of impact problems.

Material models based on plasticity can further be classified into two as follows: (a) elastic-perfectly plastic and (b) elastic plastic with kinematic hardening. Both material models are used for analysis system where a system is allowed to yield plastically; then a restoring force is likely to be as illustrated in Figure 4 a and b. As shown in Figure 4, it is evident that to some extent a material deforms elastically in linear elastic region where then a plastic yielding makes the curve extend with no slope (elastic-perfect plastic) and reduced linear slope (elastic-plastic with kinematic hardening). For both cases, when a structure is unloaded, the behavior is restored in elastic limit unless further reverse loading produces compression plastic yielding Paz [40].

During analysis of structures under combined blast-impact loads, influence of stress rate in elastic-perfect plastic material mode can be taken into consideration by increasing yield level according to ultimate stress. Likewise, rate effects upon yield surface of an elastic-plastic with kinematic hardening material model can be introduced into analysis by employing hardening parameters.

Under domains of extreme close-range explosion events with large impactive natures of forces, fracture mechanics and damage theories are introduced. Fracture mechanics is clustered into two divisions as linear and nonlinear. The linear theory of fracture provides a basis to predict unstable or catastrophic crack propagations, whereas study on amount of energy consumed in plastic or microcracked process zone is more relevant in nonlinear fracture theory [39]. Damage theory basis principle where such conditions occur when there is an irreversible degradation of material under deformation is reached.

3.2. Dynamic Strength of Materials. A structural element prone to accidental loads such as combined blast-impact loads elucidates a higher strength in material strength than a similar element subjected to static load [1]. This increased stresses or dynamic strengths are used to compute the element's dynamic resistance to applied extreme load.

Typical stress-strain curves for concrete and reinforcing steel are shown in Figure 5. Solid curves represent stress-strain relationship for materials tested at strain and loading rates specified in ASTM Standards at static case. At a higher strain rate, as represented by a broken line, dynamic materials strength is greater as compared to static test results [1, 29].

From the standpoint of structural behavior and design, the most important effect of strain rate is increased yield and ultimate strengths of reinforcement and compressive strength of concrete. For typical strain rates encountered in reinforced concrete elements subjected to accidental loads, increase in yield strength of a steel and compressive strength of a concrete is substantial. The fast-loading rate results in a significantly higher yield strength of reinforcement, whereas ultimate strength of reinforcement is much less sensitive to strain rate. The increase in ultimate strength is slight, and strain at which this stress occurs is slightly reduced. There is essentially no change with strain rate in modulus of elasticity and rupture strain of a steel. In case of concrete, it is observed that compressive strength of concrete is greater under rapidly applied extreme load. On the other hand, as strain rate increases, scant modulus of elasticity increases slightly, and strain at maximum stress and rupture remains nearly constant (Figure 5).

4. Response and Failure Modes

A structural response to blast loading depends on the ratio of blast loading duration (t_d) and fundamental vibration period of the structure (T) [41]. When the ratio (t_d/T) is very small,

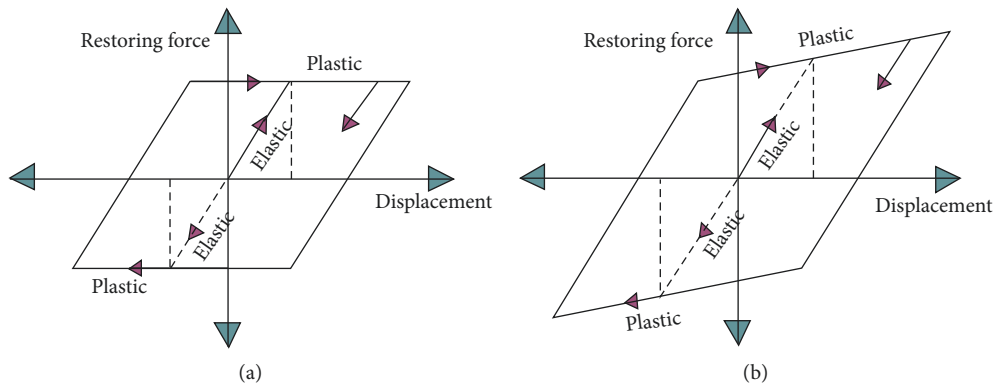

Figure 4: Elastoplastic material models: (a) elastic-perfect plastic model and (b) elastic-plastic with kinematic hardening.

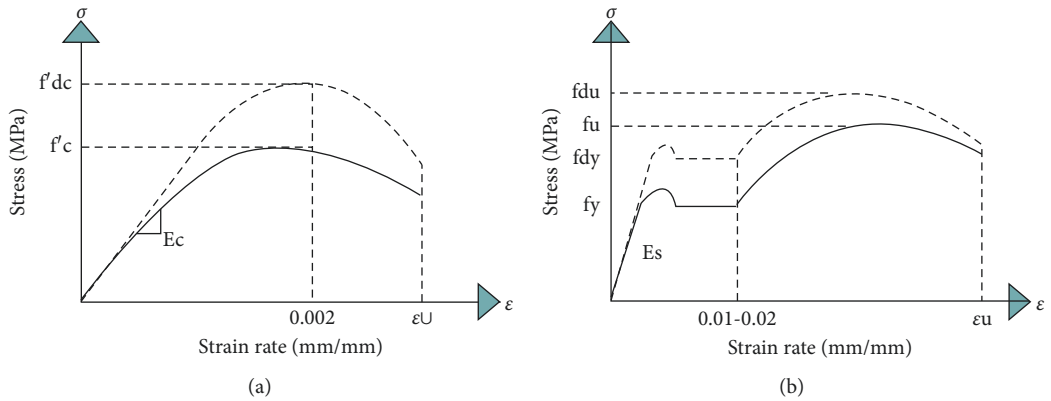

Figure 5: Stress-strain curves: (a) concrete and (b) reinforcing steel.

the loading system is in an impulsive state; thus structural response will depend on induced stress and structural mass resists applied load. Conversely, if the ratio is large, the states of stress is in quasi-static mode and structural stiffness takes the response. Also, if the ratio of blast loading duration (t_d) and fundamental vibration period of the structure (T) is equal, then the state of stress is in dynamic loading scheme and in this case, all structural responses depend not only on inertia and stiffness but also on damping [41].

4.1. Response of Structures under Blast Load. Many researchers including [42–47] evaluated response of a RC column subjected to blast load and concluded that severe effect of blast induced shock wave on columns depends on parameters such as scaled distances, geometry, presence of axial load, and detailing schemes. Similar studies on steel columns [48–51] urge use of SDOF analysis to capture influence of axial load ratio and strain rate effect. On the other hand, despite associated risk and expensiveness of experimental works, some researchers [52–54] reported experimental work on RC columns prone to explosion. The researchers outlined close-in and contact detonations cause severe damage including direct shears, spalling, scabbing, and perforation. Magallanes et al. [5] presented an experimentally reported data on steel columns. Experimental work on effect of underwater explosions on RC columns was also conducted [55, 56] and the researchers reported scaled distance and location of charge mass had vast influence on severity of respective damage modes.

Response of RC beams when subjected to blast load was investigated numerically by few authors [42, 57, 58]. The authors gave emphasis on effects of strain rates, time-dependent stiffness degradation factors. Analytical study using Euler–Bernoulli and Timoshenko beam theory were performed to characterize impacting loading response [59, 60], as well as experimental tests [61, 62]. The researchers reported effects of scaled distanced, reinforcement ratios on limit of damage modes (failure types). On the other hand, dynamic response of slabs loaded with blast induced shock waves were also studied numerically by various researchers [63–69]. The authors revealed results on cracks formations, ways of retrofitting (strengthening) techniques, and strain rate effects. Besides, the effect of explosions on RC walls was also studied numerically by some researchers including [70–72]. The researchers used SDOF method of structural analysis as a means of preliminary analysis and suggested the method for rough estimations.

Many researchers studied behavior and dynamic response of RC bridge columns and piers subjected to blast loads. Researchers [73–84] studied effect of blast loads under different parameters including scaled distances, blast load

types, presence of different superstructural axial loads, different location of explosives along height of piers, strain rate effects, and respective damage mitigation techniques.

In previous studies [85–88], considerations were also given for study of entire frame system of a buildings and bridge structures under synergetic effects of combined blast-impact loads resulting partial or total progressive collapse. These studies offered peek into blast and impact loading fragility of a structure in global and local level with specified probability to failure. After separating FEA models with typical class, capacity, and performance criteria, failure probability of a multi-story framed building was evaluated by using a key performance indicator [85–87]. This type of probabilistic risk analysis enables the researchers to trace and capture different fragility levels and respective damage states of framed structures. In addition to this, Kumar and Matsagar [88] determined blast fragility and sensitivity of a steel braced ordinary moment resisting frame system. After employing Kinney and Graham's approach, the authors proposed different blast scenario with surface blast origins and argued sensitivity case of standoff distance on behavior of blast fragility of moment resisting frames.

Computational models of framed structures prone to extreme loading induced effects, especially progressive collapse cases, were investigated by a few authors [89–91]. A study on failure probability of a steel frame systems against extremists attack from a planned explosion case was conducted by Ding et al. [89]. After developing a 3D nonlinear macro-based model with 10 stories, the researchers were able to predict and trace the failure propagation of the system. Likewise, the authors in [90, 91] conducted a stochastic analysis for a 10- and 30-story framed building against progressive collapse induced by abnormal loads by using both probabilistic and deterministic analysis methods. When comparing the conventional deterministic with probabilistic analysis, results from numerical analysis revealed the former one is sufficient and effective to capture collapse event predicted by DOD [1] with probability of 5%. On the other hand, for some sensitive RC buildings with low collapse risk, probabilistic analysis was found to be preferable.

The failure modes of a structure subjected to blast induced shock wave mainly depend on both explosive loading parameters (overpressure, time duration, and impulse) and structural characteristics (geometry, boundary conditions, and material properties). Researchers [8, 41, 92] presented local and global damage profiles for a reinforced concrete member subjected to blast induced shock waves. According to Appuhamilage [92], global and local failure modes depend on scaled distances. For a small-scaled distance blast scenarios, a compressive stress with large magnitude hits front face of a structure and travel though thickness of then medium which in turn reflects at the back face resulting in local failure modes including spalling, scabbing, and perforation (Figures 6(a) and 6(b)). On the other hand, for a far-field explosion events, blast load can be assumed to be uniformly distributed and when this uniform pressure is applied on impacted face of a structure, some induced global failures such as flexural and shear failures can be observed. In cases of flexural failure modes, a structure is associated with plastic hinges (Figure 6(c)). In contrary, shear failures are associated with less significant deformations but large breakage of intact element around supports revealing a direct shear (Figure 6(d)).

Furthermore, Gholipour et al. [6] illustrated a damage profile for a bridge column under different blast loads (Figure 7). In their research, the authors revealed shear failure modes commonly absorbed when bridge columns are prone to small scaled distance blast scenarios. whereas flexural mode of failures incurred for large scaled distance blast loading cases.

4.2. Response of Structures under Impact Load. The effects of impact load on beams and columns were studied numerically by various authors [93–101]. Impact velocity, mass, and use of composites were parameters taken for their study and crack patterns and damage modes were extracted and presented in their research articles. On the other hand, researchers [102, 103] revealed an experimentally reported data on response and performance of RC slabs subjected to impact load. Similarly, numerical studies [104–109] and experimental studies [110–117] on RC slabs under low-velocity impact loading scenario were investigated. Furthermore, mass concrete [118, 119] under impact load accompanied by different strain rates was also studied.

Recent numerical studies on impact load caused by either vessel or vehicular truck collisions on bridge piers were investigated by a few researchers [120–125]. The research parameters included by the aforementioned authors include impact velocity, mass of striker, different strength of materials, and uses of composites. In their result, the researchers reported different findings on crack width, patterns, and failure types of bridge piers.

Structures prone to impact load reveal different failure mode when compared with other loading cases such as static loads. Various authors [8, 105, 109, 112, 117] presented local and global damage profiles for a reinforced concrete member subjected to impact load. In their study, the authors concluded that severity of damage mainly depends on impactor's velocity and drop weight. The local damage failure modes were created by stress wave propagation responses, i.e., on contact point of a striker and struck body (Figures 7(a) and 7(b)), whereas global failure is mainly caused before an impactor penetrates a structure and this type of failure may result in onset of cracks with irregular paths on compression and tension zones which finally grows to global shear and flexural damage (Figures 7(c) and 7(d)). In other words, tensile cracks are formed by tensile flexural stresses and they can be mapped when in-plane normal stresses exceed concrete tensile strength.

Furthermore, Gholipour et al. [6] presented a damage profile for a bridge column under different impact loads (Figures 8 and 9). According to the researchers, shear failure modes commonly take place when bridge columns are prone to high velocity impact loads. On the other hand, combined flexural-shear and flexural mode of failures are responsible for collision loads with lower impact velocities.

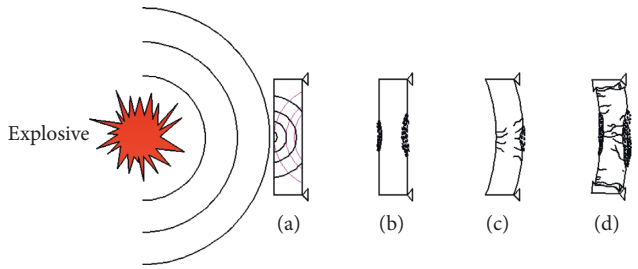

Figure 6: Blast response of RC member: (a) transmission of stress wave; (b) local damage points; (c) global flexural failure; (d) global direct shear failure.

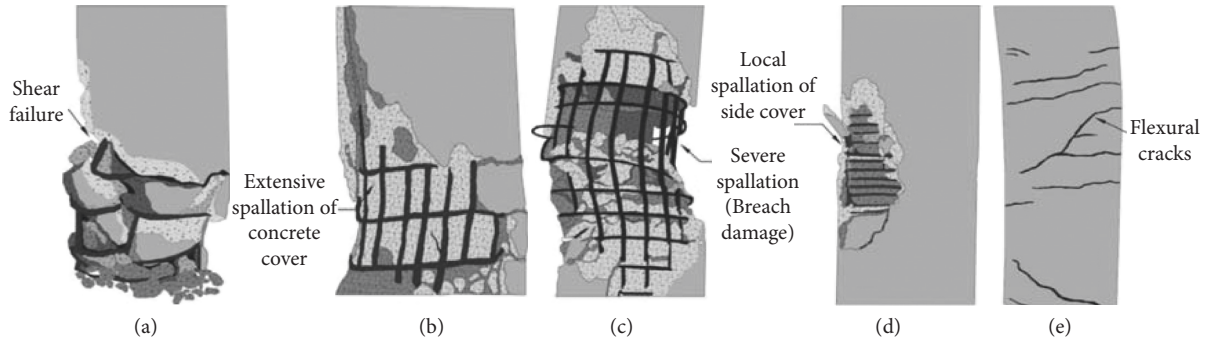

Figure 7: Typical failure modes of RC bridge column under blast load [6]: (a) brittle shear failure; (b) medium spall damage of concrete cover; (c) severe spall damage; (d) local spall damage of concrete cover; (e) flexural failure.

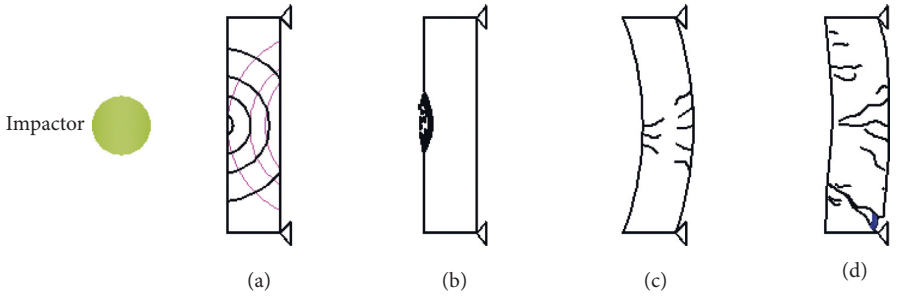

Figure 8: Impact response of RC member: (a) transmission of stress wave; (b) local damage point; (c) global flexural failure; (d) global shear failure.

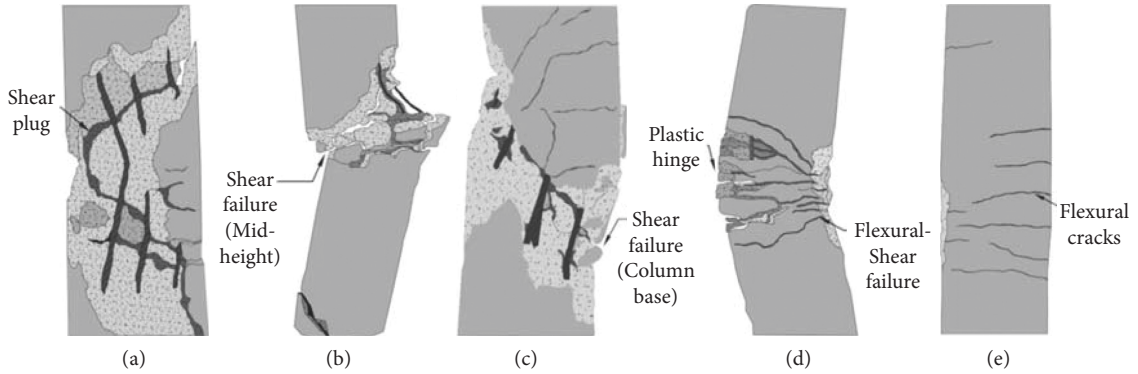

Figure 9: Typical failure modes of RC bridge column under impact load [6]: (a) punching shear; (b) shear hinge; (c) diagonal shear failure; (d) combined flexural-shear failure; (e) flexural failure.

4.3. Structures under Combined Blast-Impact Load. The response and failure (damage) modes of structures depend on both loading and structural characteristics, which can be classified into two, namely, global and local failure modes. The type of failure (damage) mode also depends on explosive characteristics, material strength, boundary condition, geometry, and speed of impactor (impact velocity).

The means for initiation of spalls on RC member describe the propagation of stress waves into two phases, namely, compression wave and tensile wave propagations. In other words, when an explosive material is detonated and results in large shock wave accompanied by an impactor fragmented body that strikes a given wall, then a compression wave is induced to the system and travel up to free end of a concrete member at rear side; respective counterbalancing stress is bounced back which is termed as tensile wave propagation stages. Thus, based upon magnitude of the load, researchers insisted creation of small cracks (small magnitude) and severe damage spallation (large magnitude). Here, researchers [3, 6–10, 27] claimed such kind of spallation is a means of difference between compression and tension capacities of concrete.

4.4. Beams and Columns under Combined Effects of Blast and Impact Loads. Reinforced concrete beams [8–10] and columns [6, 7, 11] were explicitly investigated under synergetic effects of combined blast and impact loads. Zhongxian and Yanchao [12] also developed a new method for progressive collapse analysis of framed building structures prone to blast and impact loads.

Gholipour et al. [8] proposed a novel literature implying damage indices on basis of residual flexural and shear capacities of a RC beam member. The researchers examined sensitivity of specimens under different combinations of loading schemes. Since there was no experimentally reported data on the synergetic effects of combined effects of blast and impact loads on RC beam, the aforementioned researchers argued to validate the numerical model by using a separate experimental specimens tested individually for blast and impact loads, respectively.

In their study, the authors reported sever damage, especially spall-off failure type emerged when impact loading was allowed to strike first before induced shock wave strikes a beam. Furthermore, extra severe damage and large residual displacement were observed when an explosion event was designed to act at exact time of peak-displacement of a beam. Moreover, the proposed shear and flexural failure damage indices were found to be dependent on parameters including striking velocity and loading sequences.

Gholipour et al. [9] evaluated nonlinear dynamic behavior and damage modes of a simply supported RC beams subjected to combined impact-blast loading. Similar to [8], this study was conducted by considering different combined loading scenarios with different sequences and respective time lag. Among from available different rate of impacts (low, middle, and high rates), a middle-rate impact load and moderate-explosive energy loading case were designed to be imposed to mid-height of a beam. When blast induced shock wave hit a beam prior to a striking impactor body, a local damage typically spalling type of failure was detected at concrete cover zones of a beam and global direct shear failures generated at supports. Conversely, when an impactor struck an RC beam before an explosion was detonated, critical local damage (spalling) and large displacement were observed. In addition to different parameters, the researchers [9] studied effect of time duration for impactor. From this point of view, their FEA result showed more severe damage and large-residual displacements emerged for time when an explosion was allowed to be detonated on exact time of free vibration stage of a specimen.

In reinforced concrete structures, a strain compatibility theory (perfect bond) is assumed at onset of analysis. But this assumption may lead to erroneous computations unless it is evaluated for different type of load cases and bond-slip effect was considered in numerical computations of structures under combined blast-impact loads. Thus, by introducing a new numerical model which was designed to consider effect of bond-slip between reinforcement and concrete, Kwak et al. [10] investigated the effects of combined blast-impact loads on RC beams. According to Kwak et al. [10], the effect of bond-slip can be easily captured by using the equivalent bending stiffness of a member placed around the plastic-hinge locations and this method of analysis was validated by experimental data. Based upon correlations obtained from this study, the researchers emphasized taking into account of effects of bond-slip.

By proposing three different damage indices, Gholipour et al. [6] evaluated damage level of a bridge column under synergetic effects of combined blast-impact loads. In addition to this, type of impactor (vessel type), impact velocity, and time lag were also investigated. The authors considered two RC girder bridge column with two hollow-section columns and two typical vessel varying bow configurations. Then vulnerability assessment of bridge columns under synergetic effects of blast-impact loads was conducted under sole blast, impact, and combined loading cases. Also, Gholipour et al. [6] deployed three damage indices namely residual axial load, shear force, and flexural moment capacities of the bridge column. From numerical analysis results, combined blast-impact load revealed more severe damage on bridge column than sole blast or impact loads. Moreover, larger damage indices were obtained for a barge-pier column collisions than ship-pile's cap collisions. Bridge column suffered greater internal forces and displacement values when sequential blast load was applied simultaneously with happening of time of peak impact force. Damage profiles of bridge column under synergetic effects of combined blast-impact loading case are depicted in Figure 10.

Gholipour et al. [7] numerically investigated synergetic effect of combined blast and impact loading cases for axially loaded RC columns. Since there was no experimentally reported data on combined effects of blast and impact loads on RC column, the researchers were obligated to validate the numerical model by using a separate

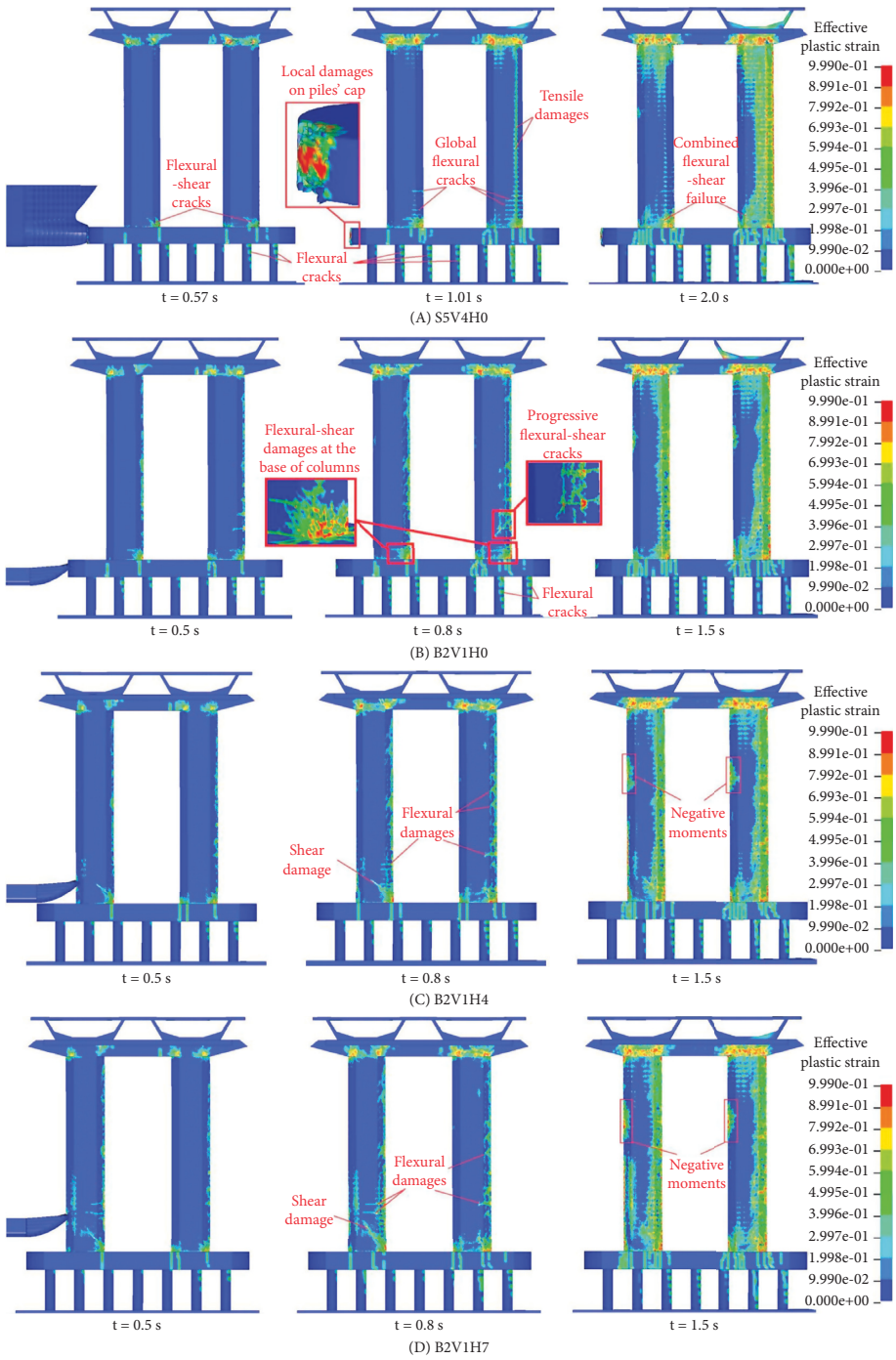

(a)

Figure 10: Continued.

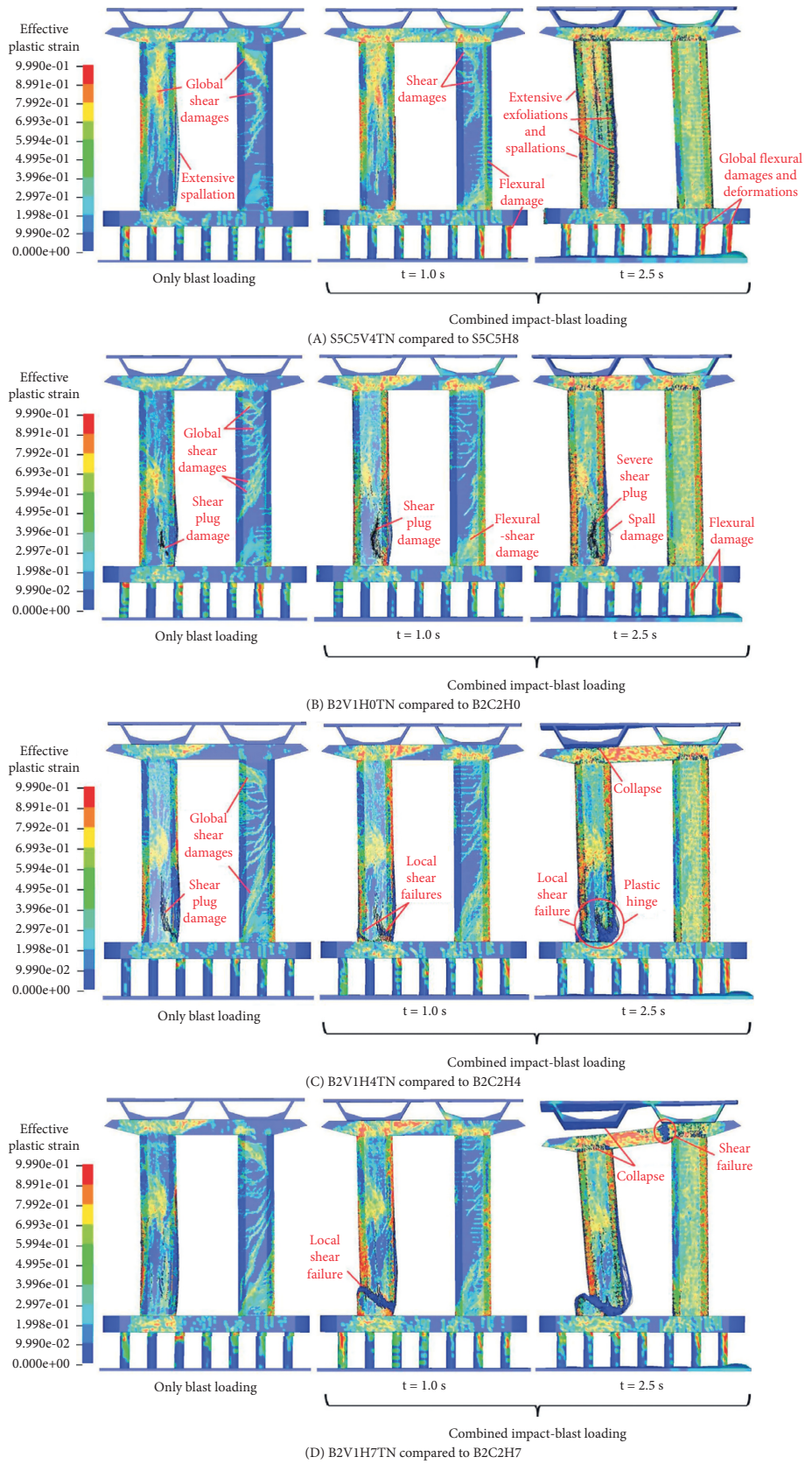

(b)

Figure 10: Summary of FEA numerical simulation failure modes for RC bridge column [6]: (a) different location of loading; (b) only-blast and combined loading effects.

experimental specimens tested individually for blast and impact loads, respectively. To capture different effects of combined loading scenarios, the researchers considered different parameters such as loading sequences, time lags, striking velocities, and presence of different axial load ratios. To estimate the extent of damage caused by combined effects, a multi-step loading procedure damage index value was deployed. Moreover, a simplified numerical model was proposed to trace location of plastic hinges of studied RC column. To create a stable state, axial load induced to the system was applied as a ramp which was designed to be greater than the first periodic time of the study column.

From the FEA study results, Gholipour et al. [7] remarked the column was susceptible to severe damage when a striking body and explosive materials were located at the same coordinates. For large scaled distances, severe local damage, especially spallation, was observed for the impact-blast loading scenario. Large global failures were traced to happen when sequent blast load was initiated at the exact time of initial peak striking force. Furthermore, Gholipour et al. [7] articulated ALR with 0.3 threshold value for RC columns prone to combined actions of blast and impact loads. Tables 2–6 present effects of numerous parameters and failure types in the study of RC beams and columns under combined blast-impact load, respectively.

Krishnan and Nair [11] conducted a numerical study on dynamic response of short and long reinforced concrete column when subjected to combined blast and impact loads. For the development of the FE models, the researchers employed ANSYS 19.2. Solid 185 and beam elements were used for the modelling purpose concrete and reinforcement bars. Krishnan and Nair [11] conducted a parametric study and parameters including shapes of a column (square, rectangle, and circle), aspect ratio (column length and width ratio), longitudinal reinforcement ratio, and spacing of transverse reinforcements. Among the three different column cross-sections of RC column prone to combined blast and impact loads, circular columns revealed lesser displacement and damage values. From the FEA analysis result, it is insisted that increasing reinforcement ratios significantly drops displacement values. In addition to this, short RC columns with minimized tie spacing displayed a significant role in withstanding the combined blast and impact load effects. Summary of parameters, damage profiles, and respective synergetic effects of combined blast and impact loads on beam and columns are depicted in Tables 2–5.

Moreover, Li and Yanchao [12] proposed a new method for progressive collapse analysis of RC building. The proposed method is accompanied by three stages. First, critical blast-impact scenario is delineated. Second, non-zero initial conditions and initial damage of the structural members are derived. Finally, a numerical analysis of structural progressive collapse with non-zero initial conditions and damaged structural members is conducted. The authors claimed that the new proposed method which accounts for non-zero structural conditions and does not require a comprehensive modelling of a structure under synergetic effects overcomes the disadvantage of conventional analysis method.

4.5. Slabs, Plates, and Walls under Combined Effects of Blast and Impact Loads. A few studies [13, 14] investigated the dynamic effects of combined blast-impact load on RC slabs. Likewise, the authors [3, 15–18] numerically and experimentally studied combined effects of blast and fragment loading on walls. Also, the researchers [19–25] studied combined blast-impact loading scenario on different panels with composites and laminates. Furthermore, the combined effect of aforementioned loading scenario was also investigated on mass concrete by some researchers including [4, 26, 27].

Tao et al. [13] experimentally and numerically investigated damage characteristics of RC slab prone to combined blast and fragment load cases. The study RC slab had 40 mm thickness and was designed to be loaded with blast induced shock wave and respective fragments. The authors used a nonlinear dynamic computational program AUTODYN's smoothed-particle hydrodynamics (SPH) method to trace and capture fragment loads. Furthermore, the authors proposed empirical formulas to characterize RC slab damage prediction. In their experimental test results, the researchers revealed for large scaled distance RC slab panel was exposed to damage limited in minor zones. In contrary, for a combined blast-impact load scenario accompanied by close-ranges, RC slab was observed to be susceptible to large holes and craters. Consequently, their numerical simulation results exhibited a large effect of scaled distance, i.e., explosive charge mass and standoff distance.

Linz et al. [14] numerically evaluated damage paths and failure types of a reinforced concrete slab. The generated FEA model was validated with both experimental and analytical methods and using the advantage of symmetry, only quarter size scaled FEA model was employed throughout their study. The nonlinear explicit FEA packaged program LSDYNA was used to trace damage extents, crack patterns, and shrapnel effects of fragments. In order to create a stable solution, the researchers deployed two-step systems on which striking body was allowed to hit the slab within 50 μs and then by clearing the remaining fragments, a successor load (blast induced shock wave) detonated with 10 ms time of duration. The study claimed importance of considering fragment speed intensity. In other words, when fragment speed was increased from 1650 m/s to 1780 m/s, a significant damage and different sized craters was obtained.

Likewise, numerical studies on combined effects of blast and fragment loading on RC walls were conducted by [3, 15–18]. The response of reinforced concrete slab when subjected to combined blast and fragment loading was studied by Sepncer and Wei [15]. The researchers deployed a numerical computational method accompanied by a nonlinear FE packaged software LSDYNA and for use of material data, C-35 concrete and S-460 rebar were taken into account. Spencer and Wei [15] explicitly evaluated synergetic effects of blast and fragment loadings on different arrangement of rebars and boundary conditions of RC slab. After extracting and analyzing postprocessed data from LSDYNA, the researchers inferred increasing number of reinforcement bars in a RC slab and imposing a fixed boundary condition enables the slab to absorb enormous damage and displacement values.

Table 2: Summary of different parameters and respective effects on RC beams subjected to combined blast and impact loads.

Author (s)	Analysis method	Parameter lists	Remark
Gholipour et al. [8]	FEA (LS-DYNA)	Reinforcement configurations (i) Low shear (L22S6) (ii) Low flexure (L12S12) (iii) Sufficient shear-flexure (L22S10)	Increasing the rate of impact from 2 m/s to 12 m/s, makes specimen failure mode in shear and flexure
		Loading sequences (i) Impact-blast load (ii) Blast-impact load	Impact-blast and blast-impact load scenario revealed local spallation and direct shears, respectively
		Time lags (i) Low-rate impact (2 m/s) (ii) Middle-rate impact (6.86 m/s) (iii) High-rate impact (12 m/s)	Large flexural bending moments were obtained when the sequential explosion detonated at the time of peak bending moment
Gholipour et al. [9]	FEA (LS-DYNA)	Loading sequences (i) Impact-blast load (ii) Blast-impact load	Severe damage (spallation) was obtained beneath the depth of the beam
		Time lags (i) $t_L = 2.1$ ms (ii) $t_L = 5.0$ ms (iii) $t_L = 10$ ms (iv) $t_L = 20$ ms	Increasing the time lag from 2.1 ms to 20 ms revealed global shear failure mode
		Beam depths (i) $D_1 = 0.15$ m (ii) $D2 = 0.20$ m (iii) 3 = 0.25 m	Both peak and residual displacements increase when decreasing the beam depth
Gholipour et al. [9]	FEA (LS-DYNA)	Span lengths (i) $L_1 = 0.9$ m (ii) $L2 = 1.4$ m (iii) $L3 = 1.9$ m	While changing the span length from 0.9 m to 1.9 m, large flexural bending moment was obtained
		Longitudinal reinforcements (i) Low flexure (C13T16) (ii) High flexure (C20T25)	Increasing flexural steel ratio drops the damage index values and the path of damage
		Transverse reinforcements (i) Low shear ($\Phi_t = 6$ mm @ 15 cm) (ii) Sufficient shear ($\Phi_t = 16$ mm @ 5 cm)	Beam with sufficient shear detail had small spalls

Experimental investigation on dynamic response mechanism and damage propagation stages of RC wall accompanied by combined blast induced shock wave and fragmented impact loads was performed by Linz et al. [16]. Table 7 shows damage modes of experimentally tested RC wall. From experimental test results, the authors articulated the effect of combined blast and fragment loads in terms of damage evolutions. The blast load caused mainly deformation; on the other hand, impact loads was responsible for major severe local damage and craters. The combined effects of the aforementioned loads were severe in such a way that large diameter craters and spalling were observed at back face which then was accompanied by further bending deformation and diagonal cracks propagating towards supports. The authors urged the use of synergetic combined effects of blast and fragment loads in design of concrete elements.

Moreover, Nyström et al. [3] numerically studied synergetic effects of blast and impact loads on RC wall strip. Since there was no experimentally reported data on combined effects of blast and impact loads on RC wall strip, the researchers validated their numerical model by using a separate experimental specimens tested individually for blast and impact loads, respectively. The authors extracted the combination of arrival times and estimated effects of different loading sequences using single degree of freedom (SDOF) method of analysis. Figure 11 depicts displacement-time history plot for different load cases and peak displacement is obtained from combined loading scenario.

In addition to the SDOF method of structural analysis, Nyström et al. [3] deployed a nonlinear computational program (AUTODYN) with Lagrangian solver technique. By extracting displacement-time, velocity-time history, and

Table 3: Summary of FEA numerical simulation failure modes for RC beam under combined blast and impact loads [8].

Failure modes of RC beam for different loading sequences

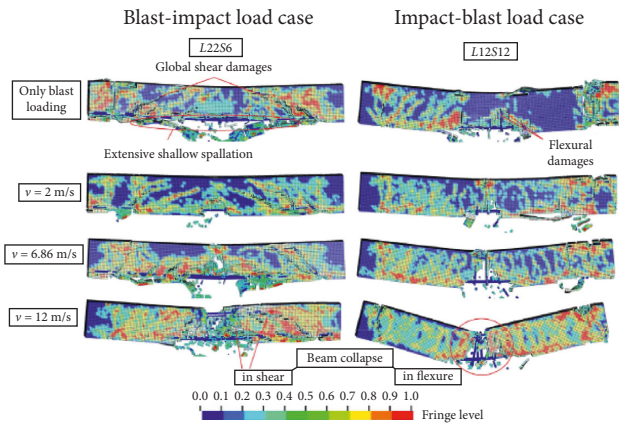

Failure modes of RC beam for different reinforcement details

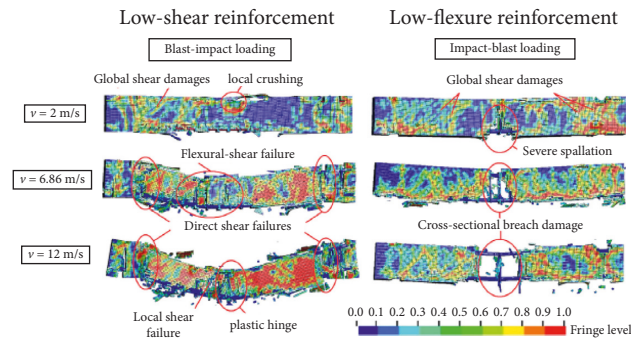

Failure modes of RC beam for different rates of loading

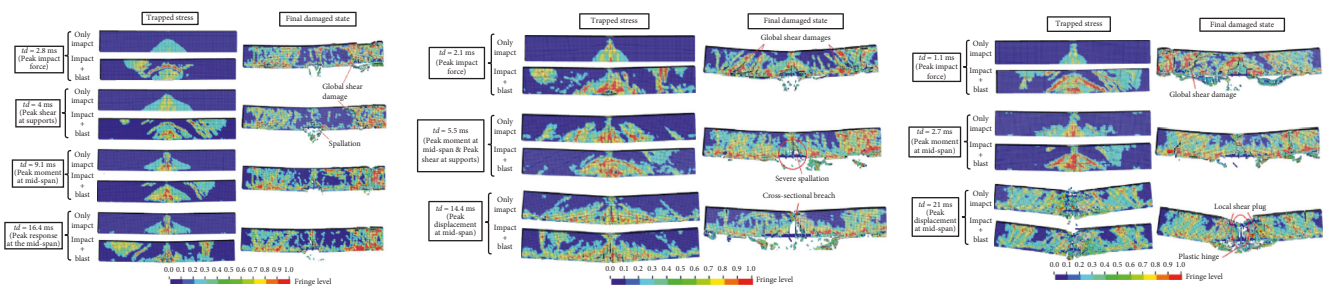

Zhang et al. [9]

Failure modes of RC beam for different time lags

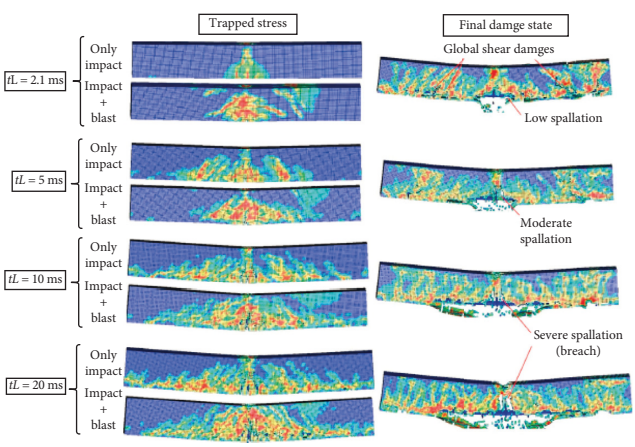

Failure modes of RC beam for different depths

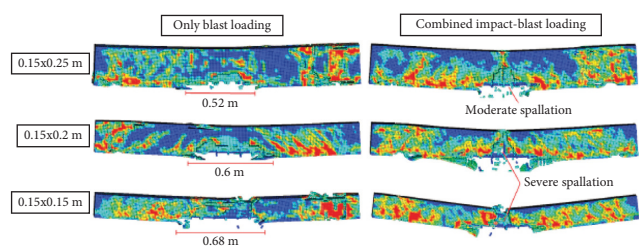

Failure modes of RC beam for different span lengths: (a) 0.9 m; (b) 1.4 m; (c) 1.9 m

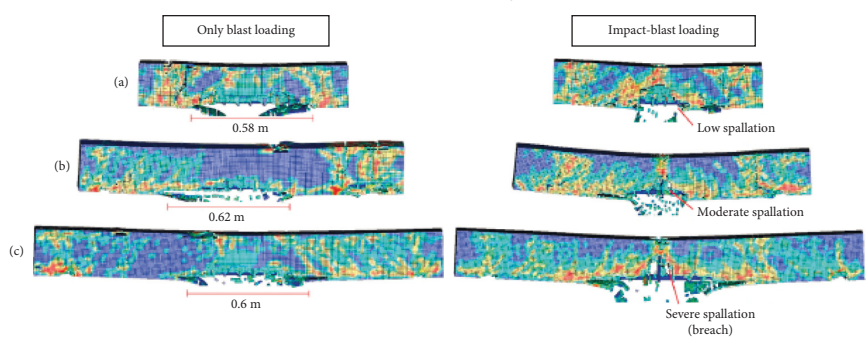

Table 3: Continued.

Failure modes of RC beam for different loading sequences	Failure modes of RC beam for different reinforcement details
Gholipour et al. [9]	
Failure modes of RC beam for different longitudinal reinforcements: (a) 0.9 m; (b) 1.4 m; (c) 1.9 m	
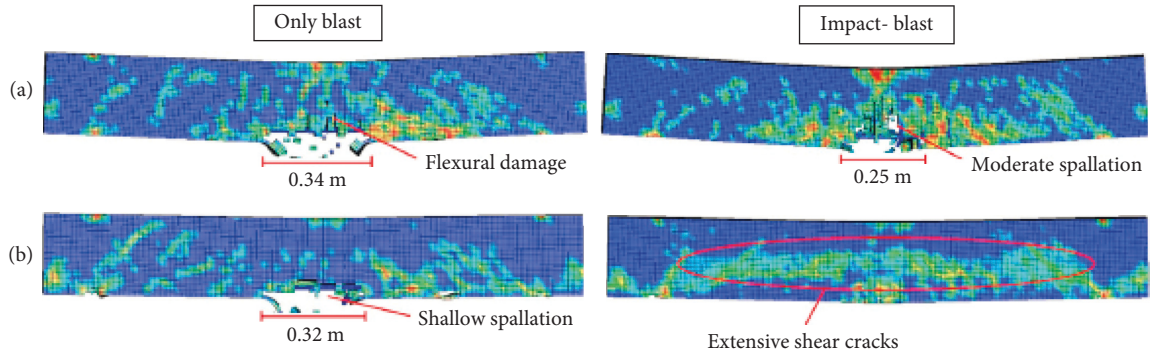	
Failure modes of RC beam for different transverse reinforcement: (a) $\Phi_t = 6$ mm @ 15 cm; (b) $\Phi_t = 16$ mm @ 5 cm	
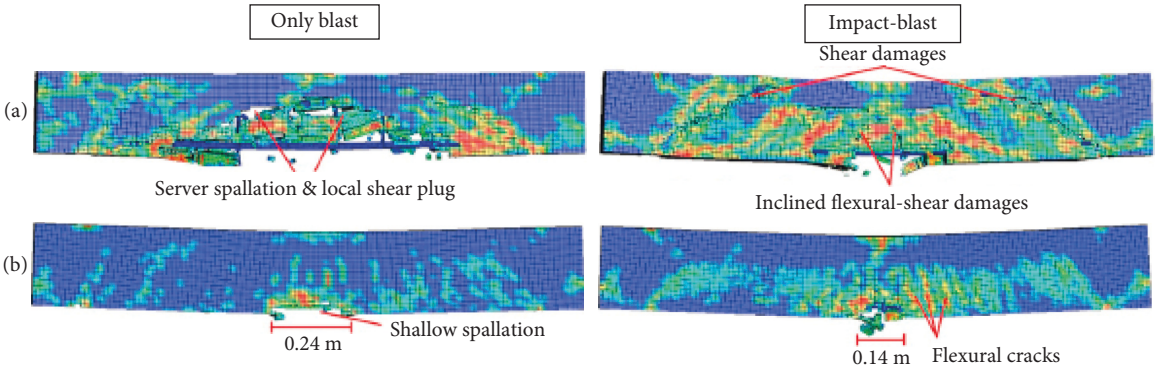	

Table 4: Summary of different parameters and respective effects on RC columns prone to combined blast and impact loads.

Author (s)	Analysis method	Parameter lists	Remark
Gholipour et al. [6]	FEA (LS-DYNA)	Loading locations (i) Ship impact on pier cap, explosion on pier (S5C5V4TN) (ii) Barge impact and explosion on pier cap (B2V1H0TN) (iii) Barge impact and explosion on lower pier column (B2V1H4TN) (iv) Barge impact and explosion on mid pier column (B2V1H7TN)	Collapse of pier column was obtained when the barge impact and explosion happened on mid height
		Impact velocities (i) Low velocity (1.65 m/s) (ii) Medium velocity (3 m/s) (iii) High velocity (5 m/s)	Impact velocity beyond 3 m/s, the bridge column tends to fail by shear failure
		Impact velocities (i) Initiation time-1 (0.09 s) (ii) Initiation time-2 (0.8 s) (iii) Initiation time-3 (1.62 s)	Time lag shorter than 0.5 s resulted in direct shear failure. Beyond this time lag, shear and flexural failure

Table 4: Continued.

Author (s)	Analysis method	Parameter lists	Remark
Gholipour et al. [7]	FEA (LS-DYNA)	Loading locations (i) Mid-height (IMP0-BLT0) (ii) Mid-base (IMP1-BLT0) (iii) Base (IMP1-BLT1)	For near-field loading cases, localized shear failure type was obtained
		Loading sequence (i) Impact-blast load (ii) Blast-impact load	Under near-field loading events, impact-blast showed larger damage index than blast-impact load case
		Time lags (i) $T_L = 0.121$ s (ii) $T_L = 0.124$ s (iii) $T_L = 0.137$ s (iv) $T_L = 0.160$ s	Increase of time lag maximizes damage level (spallation) in the column
Gholipour et al. [7]	FEA (LS-DYNA)	Axial load ratio (i) ALR = 0.1 (ii) ALR = 0.3 (iii) ALR = 0.5 (iv) ALR = 0.8	Spall type of damage decreases until ALR reaches 0.3
		Impactor velocity (i) $V_{impact} = 1$ m/s (ii) $V_{impact} = 3$ m/s (iii) $V_{impact} = 5$ m/s (iv) $V_{impact} = 10$ m/s	Striking velocity with and greater than 3 m/s revealed the column to have a cumulative damage mode accompanied by initiation of plastic hinges and localized shear failures
Krishnan and Nair [11]	FEA (ANSYS)	Column shape (i) Square (ii) Rectangle (iii) Circle	For both short and long columns, circular column revealed 2 times lesser deflection when compared to the square and rectangular columns
		Long. reinf. ratio (i) $\rho_l = 2\%$ (ii) $\rho_l = 3\%$ (iii) $\rho_l = 4\%$ (iv) $\rho_l = 5\%$ (v) $\rho_l = 5\%$	While increasing the longitudinal reinforcement ratio from 2% to 6%, long and short RC columns minimized the deflection up to 6.3% and 6.08%, respectively
		Tie spacing (i) $S = 75$ mm (ii) $S = 100$ mm (iii) $S = 150$ mm (iv) $S = 225$ mm (v) $S = 300$ mm	For long and short columns, increasing tie spacing from 75 mm to 300 mm escalated the maximum displacement value by 13.18% and 15%, respectively

Table 5: Summary of FEA numerical simulation failure modes for RC column under combined loading cases [7].

Failure modes of RC column loaded at mid-height with middle-rate, near, and far field loading accompanied by different loading sequences

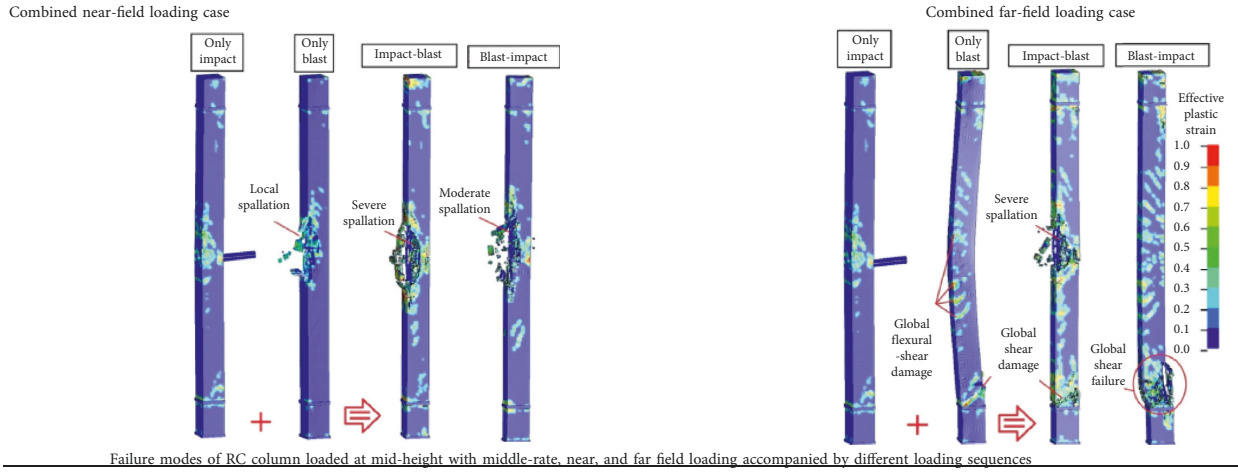

Failure modes of RC column loaded at mid-height with middle-rate, near, and far field loading accompanied by different loading sequences

Table 5: Continued.

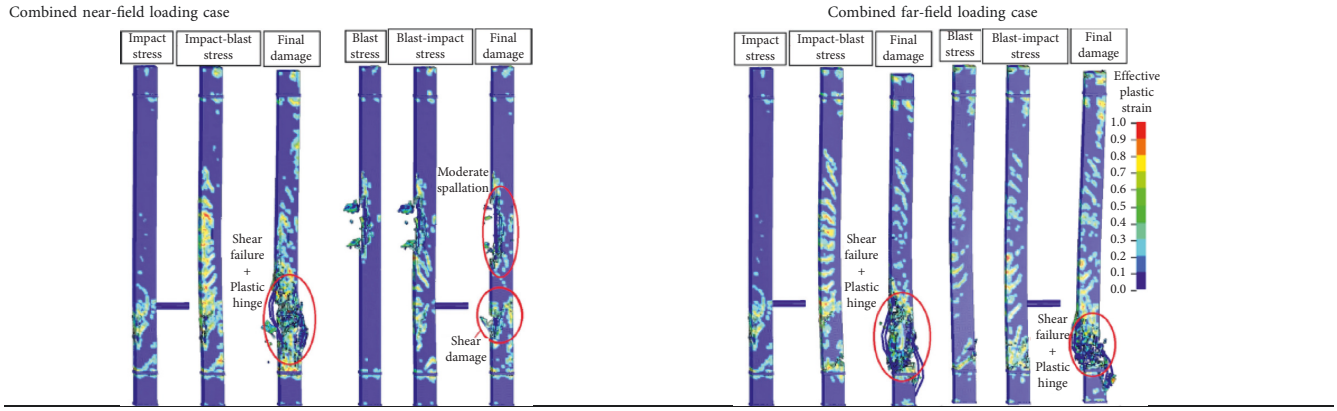

Failure modes of RC column loaded at by explosive mid and impactor at base points with near-field accompanied by different time lags

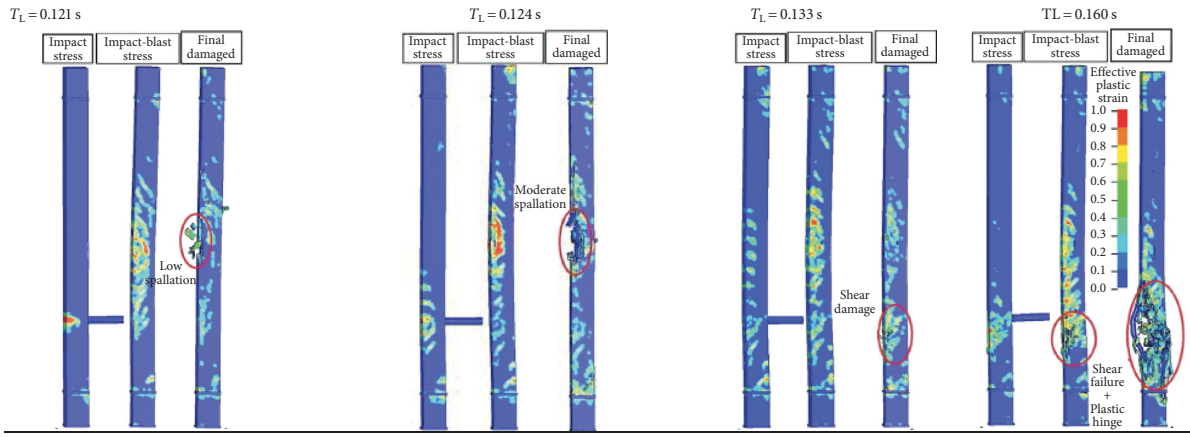

Failure modes of RC column loaded at by explosive mid and impactor at base points with far-field accompanied by different time lags

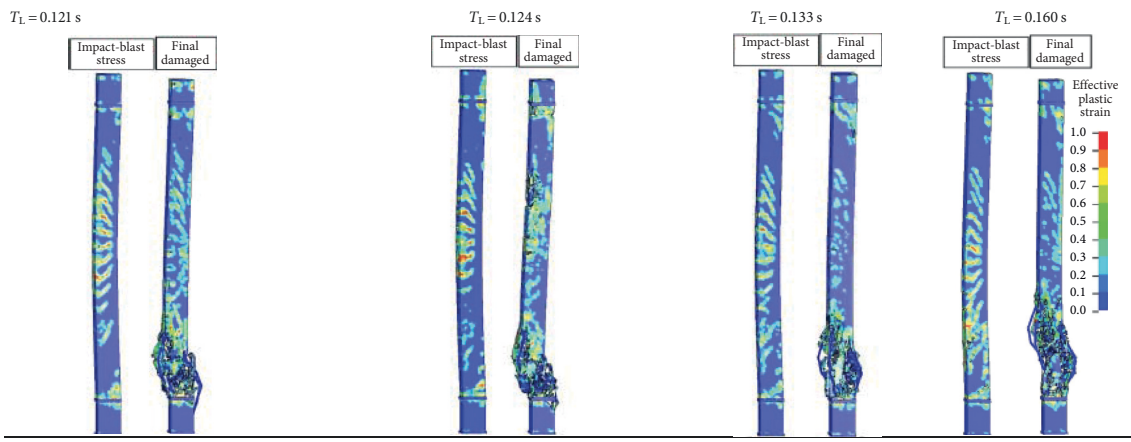

Failure modes of RC column loaded at by explosive and impactor at the mid height accompanied by different time lags

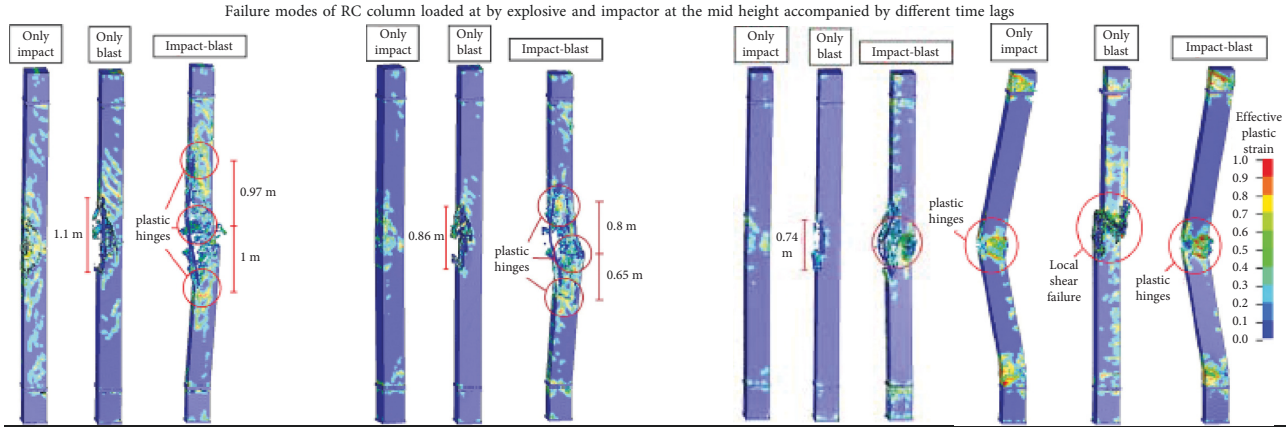

Table 5: Continued.

Failure modes of RC column loaded at by explosive at mid and impactor at the base point accompanied by different time lags

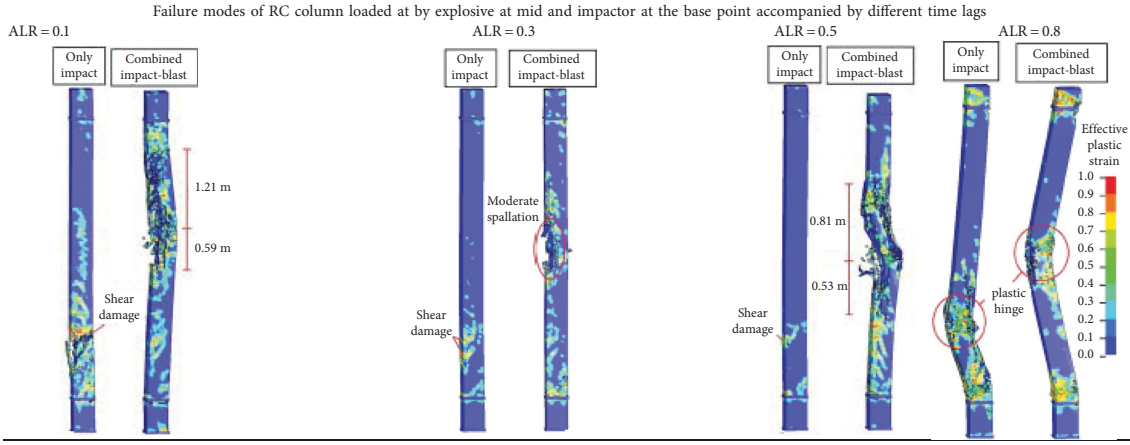

Failure modes of RC column loaded at by explosive and impactor at the mid height accompanied by different time lags

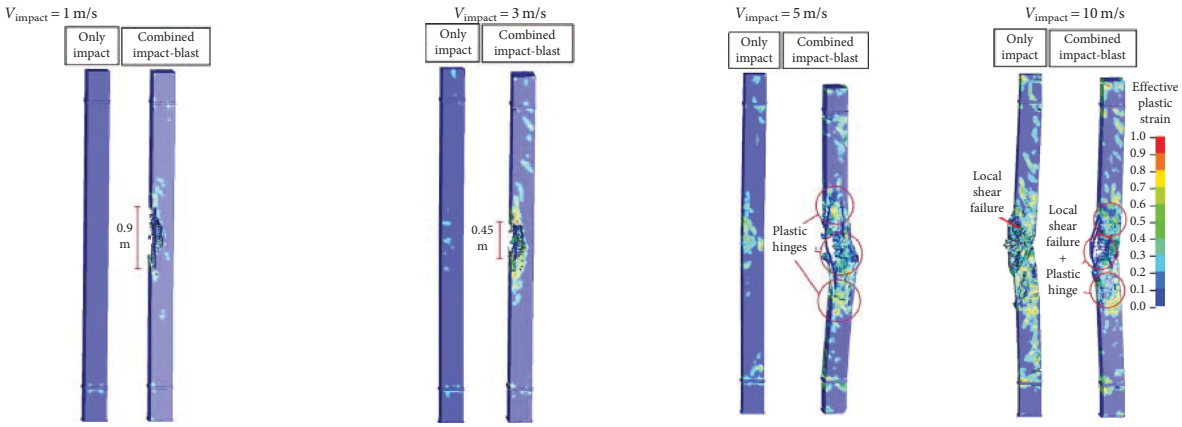

Failure modes of RC column loaded at by explosive at mid and impactor at the base point accompanied by different time lags

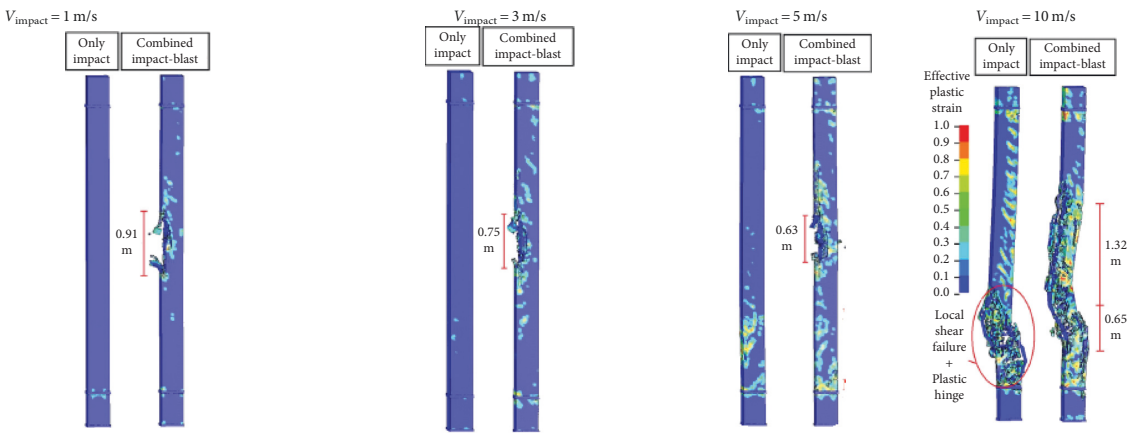

Failure modes of RC columns with different slenderness ratio loaded by combined blast and impact loads

Table 5: Continued.

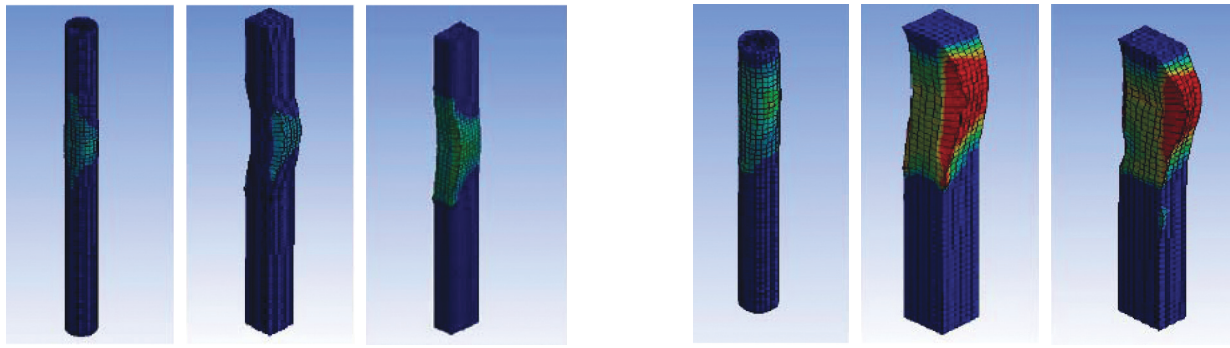

Failure modes of long and short RC columns loaded by combined blast and impact loads with 2% reinforcement ratio

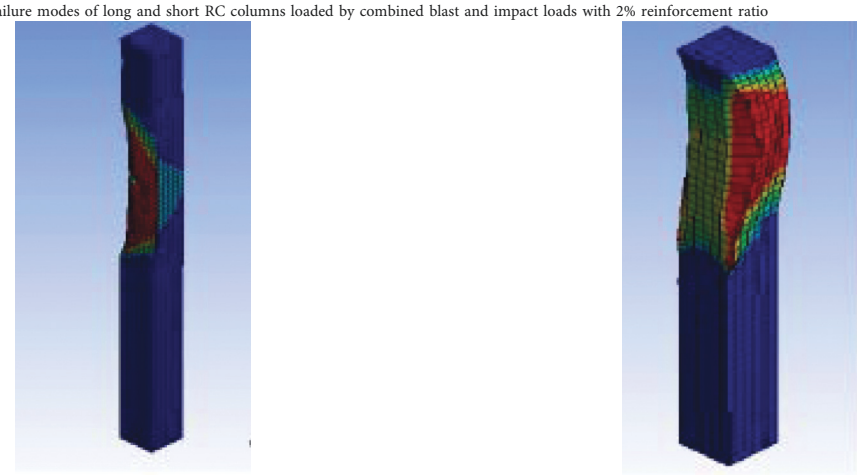

damage plots, the researchers evaluated the dynamic response of RC wall strip subjected to three loading cases, namely, (a) only blast load, (b) only fragment impact load, and (c) combined blast and fragment impact load. Figures 12 and 13 show peak nodal displacement-time and velocity-time history plot comparisons for different loading cases and from the plots, it is evident that both displacement and velocity values were observed to be dominant for combined blast and fragment impact loads. To elaborate, peak displacement for only blast loading and only fragment impacting loads was 65.2 mm and 13.3 mm, respectively. In contrast, the peak displacement value for the combined blast and impact loads was 85.7 mm.

In addition to the time history plots in Nyström et al.'s [3] study, FEA results exhibited a damage plot of specimens. Figures 14–16 illustrate failure modes of the models for different loading scenario. From Figure 14, it is clear that large cracks were formed at the rear side of specimen and yielding of reinforcements was obtained. Figure 15 depicts that a vast amount of localized damage (crater, scabbing, and direct shear crack) was retrieved from fragment impact loaded front and rear sides. For RC wall strip prone to combined blast and fragmenting impact loads and when compared to the rest load cases, localized damage especially, craters at front face and scabbing at rear side developed early which is clearly severe damage (Figure 16).

Likewise, Grisaro et al. [17] numerically evaluated the behavior of one-way RC wall subjected to simultaneous action of blast and fragment impact load. The authors conducted a novel research work that was not previously executed. Due to these reasons, it was found that design approaches of those researchers were not validated and supported with previous works. The developed numerical model was designed to account for strain rate effects. In addition to this, to trace the dynamic responses of the FEA modes, the researchers followed three-step approaches, namely, approach 1, 2, and 3. Approach 1 considered the effect of casing by minimizing specific impulse and a nonuniform spatial distribution of fragments. In contrary, approach 2 assumes uniform spatial distribution of fragments. Approach 3 was designed to neglect effect of casing. The authors' numerical simulation results showed as compared to all approaches that approach 1 was found to give a realistic detonation-fragmentation loading scenario.

Furthermore, Ekström [18] was keen to study dynamic response of RC wall prone to blast induced fragments. In their numerical simulation, combined damage and plasticity models were deployed, and use of those constitutive models assisted the analysts to easily trace real behavior of blast induced dynamic load leading spallation of concrete wall damage propagation stages. In addition to this, to evaluation effect of localized plastic strains, a smeared

Table 6: Summary of experimentally tested damage on reinforced concrete slab subjected to combined blast and impact loads.

Damage of the RC slab under blast induced shock wave and fragment impact loads [13]

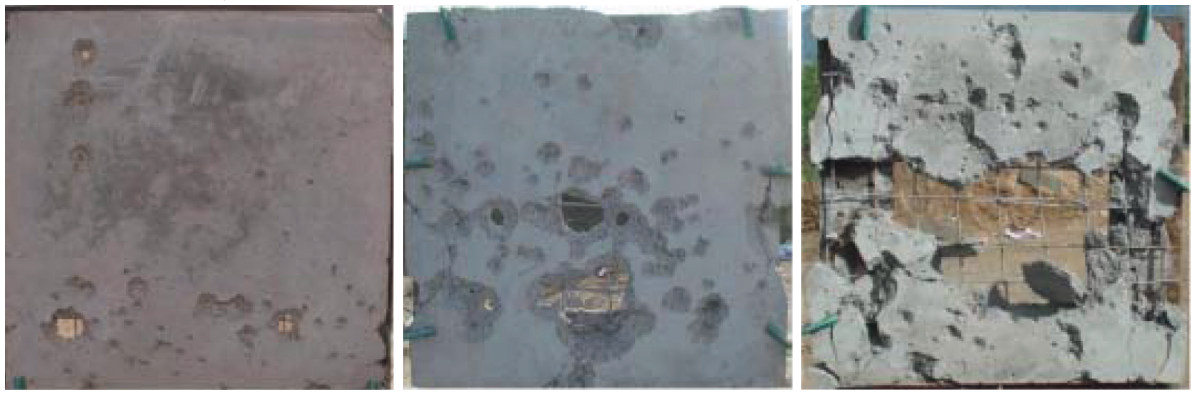

Damage and crater sizes of the RC slab under blast induced fragment impact loads [14]

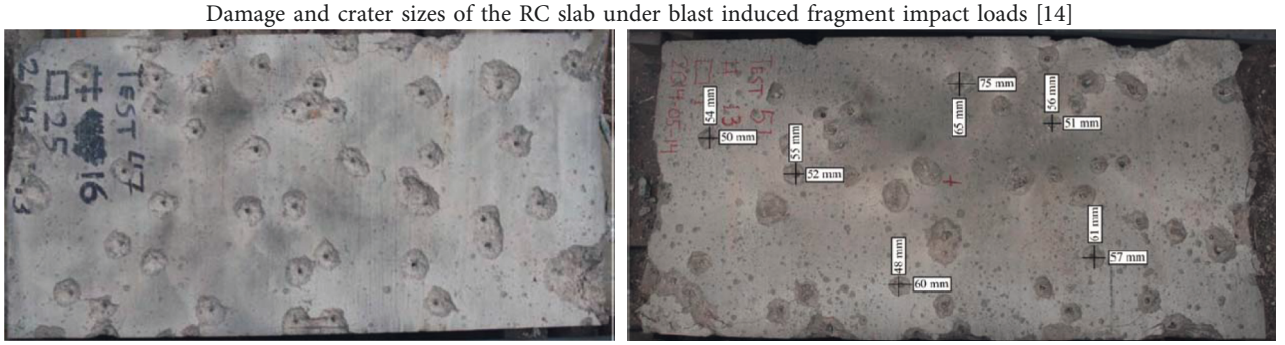

Damage of the RC slab with different rebar arrangement subjected to combined blast-impact loads [15]

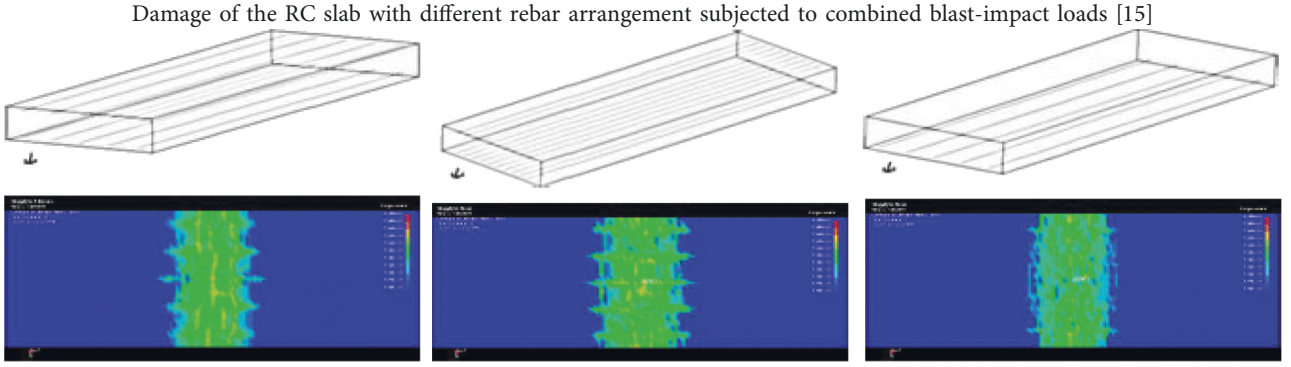

Damage of the RC slab with different boundary conditions prone to combined blast-impact loads [15]

Fixed support Pinned support

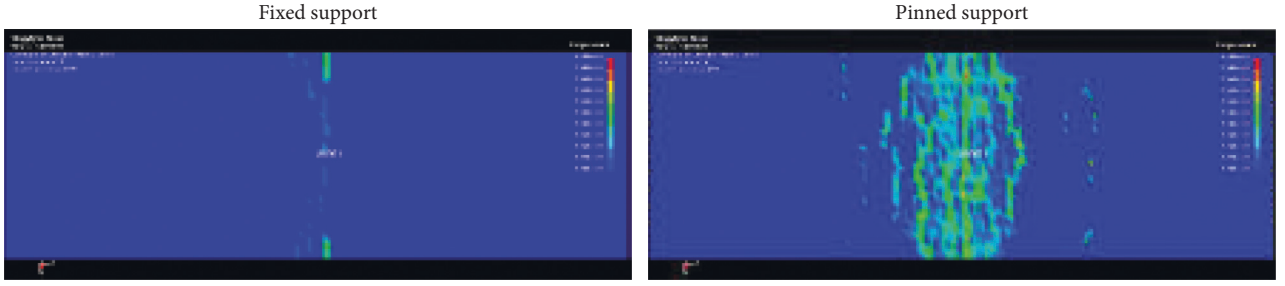

crack approach, and an explicit nonlinear 1D numerical model for uni-axial response of RC wall prone to blast induced shock waves accompanied by fragments were employed. The numerical analysis result revealed spallation does not occur when tensile strength of concrete is reached. But also, in case of cyclic response from highly dynamic loads such as blast and impact load, gradually increased plastic strains of concrete material

Table 7: Summary of different parameters and respective effects on slab panels subjected to combined blast and fragment impact loads.

Author (s)	Analysis method	Parameter lists	Remark
Tao et al. [13]	FEA (AUTODYN) and experimental	Loading sequence (i) Stage-one (ii) Stage-two (iii) Stage-three	The synergetic effect of blast-impact load made a slab to have severe damage on the back face
		Scaled distance (i) Charge mass (ii) Standoff distance	Increase in charge mass and decrease in standoff distances, creates severe damage (holes) on a slab
		Location of explosive (i) On-ground (ii) Above-ground	The explosive located on ground 4 m far from a wall yields smaller blast and fragment impulses
Grisaro and Dancygier [21]	Analytical and Experimental	Shape of fragments (i) UFC fragment (ii) Flat nose (iii) Sharp fragment	Sharp-nose shapes had larger pressure values as compared to other fragment shapes

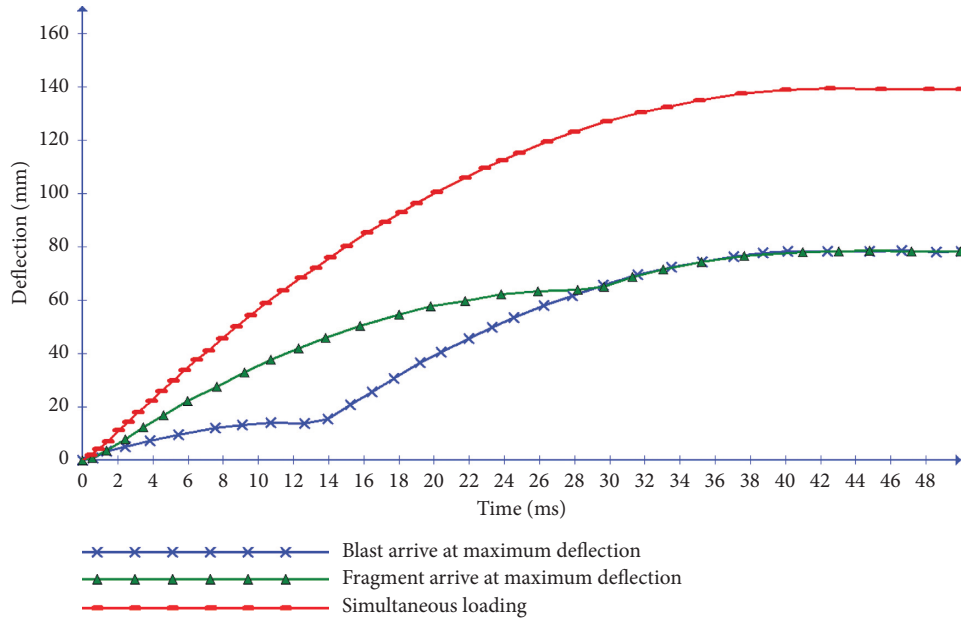

Figure 11: SDOF-based displacement-time history plot for different loading cases [3].

were observed. Table 6 lists some of experimentally reported damage modes for different members.

Recent studies on structures designed to have sufficient ductility and ability to deform in a controlled forced excitations were conducted. For instance, [19–25] examined performance of different panels with composite material formulations. Santosa et al. [19] experimentally and numerically investigated response of aluminum foam sandwiched (AFS) structures prone to blast induced fragments. Structural integrity, acceleration, and support reaction forces were extracted to evaluate blast effectiveness of proposed structure (panel). For numerical analysis, the researchers employed two blast load applying methods, namely, load blast enhanced (LBE) and smooth particle hydrodynamic methods. The LBE method was not able to capture circle-shaped perforation damage on AFS panel; thus the researchers concluded, from the available blast load modelling techniques, that the SPH method was found to be effective in giving an excellent result on failure mode.

A novel work on synergetic effects of combined blast and single fragment load was executed by Li et al. [20] where the researchers used a composite projectile system comprised of aluminum foams. Both experimental and numerical

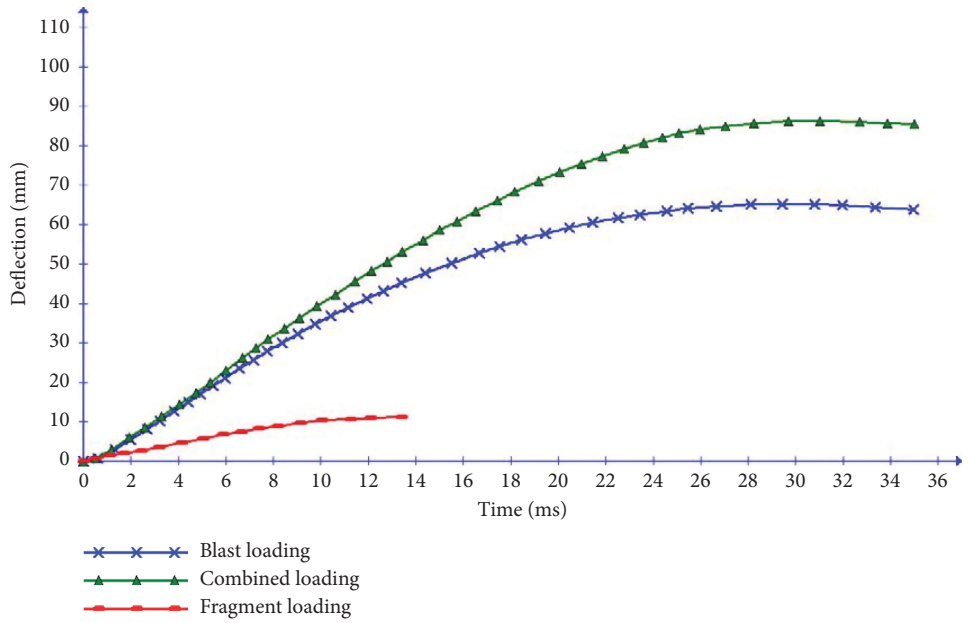

Figure 12: Displacement-time history plot for RC wall for different load cases [3].

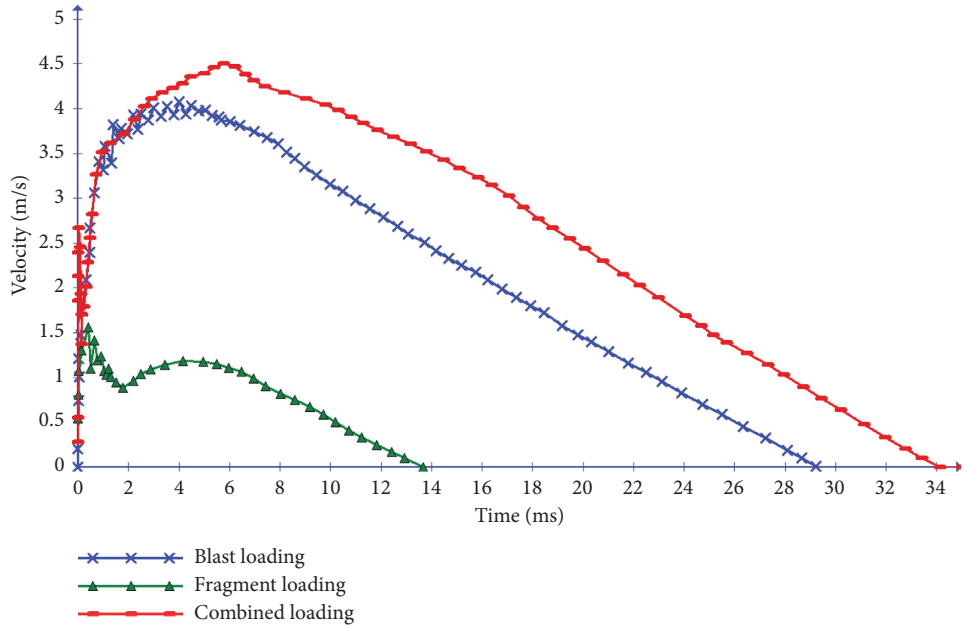

Figure 13: Velocity-time history plot for RC wall different load cases [3].

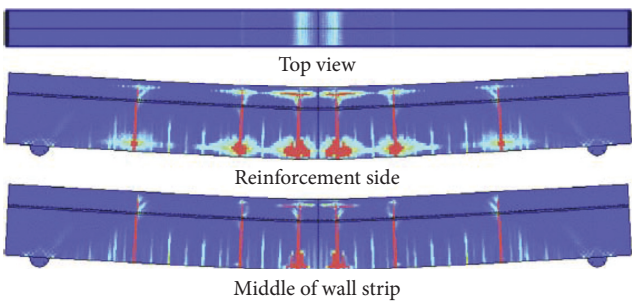

Figure 14: Damage in RC wall strip loaded with only blast load [3].

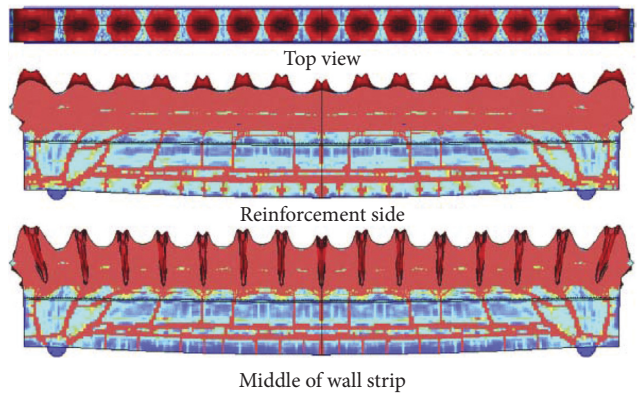

Figure 15: Damage in RC wall strip loaded with only fragment impacts [3].

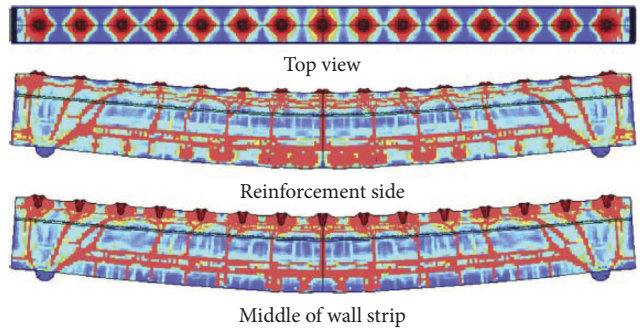

Figure 16: Damage in RC wall strip loaded with simultaneous blast and fragmented impact loads [3].

investigations were conducted to evaluate the effect of cased and uncased explosion scenarios. Li et al. [20] used a high velocity impact of very porous homogenous metal foam projectiles which can easily simulate and represent blast induced shock waves. The authors concluded that the arrival time of blast induced shock waves and single fragments plays a significant role in terms of residual velocity of clamped plate.

Similarly, Grisaro and Dancygier [21] proposed a new simplified method for multiple fragment impulse assessment of combined blast and impact loads. Grisaro and Dancygier [21] used an analytically simplified approach to validate experimental works. Though the proposed simplified approach does not trace and capture history of pressure versus time, it does give a good agreement on behalf of fragment impulses. Moreover, the authors claimed that the explosion event with large scaled distances had lower blast induced shock wave impulses and higher contribution accompanied by different shaped fragment induced impact loads.

Moreover, Santosha et al. [22] numerically evaluated a novel work on impact-blast energy loads absorption performances of a structural model with sandwich metal-foam plates. From the authors' nonlinear FEA results, displacement, velocity, and acceleration time history were extracted to trace energy absorption performance of aforementioned structural model. A parametric study on effects of foam thickness, sandwich plate configuration, foam densities, and panel material variations was conducted. A summary of parameter lists and effectiveness of the parameters is listed in Tables 7 and 8.

Nowadays, studies on protective structures subjected to blast induced fragments are profoundly important. Furqan et al. [23] studied the effectiveness of plates and stiffened plate structures for a blast induced penetrations. The researchers designed different models with and without stiffeners. The stiffener panels range from single crossed stiffener with only one and two sides of the plate. The authors performed explicit nonlinear FEA using LS-DYNA software program to evaluate impact energy absorption capacity, displacement, velocity, and acceleration time history results. Parametric study lists and respective effects are summarized in Tables 9 and 10.

Likewise, Kong et al. [24] numerically and experimentally examined combined effects of blast induced shock wave and fragment loads for metal cased multi-layer plates (cabin walls). The proposed multi-layer structure was designed to have some compartments including decks and holes on bulk head. From the experimental test, the performance and endurance of a stiffened plates were examined by utilizing deformation and rupture of a specimen. Numerical simulation was performed by utilizing AUTODYN program accompanied by coupled features of Eulerian-Lagrangian and spatial particles hydrodynamic-Lagrangian methods. From the numerical analysis results, decreasing in standoff distances increased plastic strain values of cabin walls. Even though thin-metal plate cabins were stiffened, the proposed means of strengthening was not enough to resist projectiles penetration. Moreover, numerical analysis revealed that the

Table 8: Summary of different parameters and respective effects on metal-foam Sandwich panels prone to combined blast-fragment impact loads.

Author (s)	Analysis method	Parameter lists	Remark
Santosha et al. [22]	FEA (LS-DYNA)	Single-plate (SP) thickness (i) SP 4 ($t = 4$ mm) (ii) SP 6 ($t = 6$ mm) (iii) SP 8 ($t = 8$ mm)	Increasing thickness of SP minimizes displacement values
		Sandwich metal plate (SMP) thickness (i) SMP 10 ($t = 10$ mm) (ii) SMP 12 ($t = 12$ mm) (iii) SMP 14 ($t = 14$ mm)	Even though increases in thickness of SMP significantly minimize displacement values, it was not effective in decreasing acceleration
		Sandwich foam plate (SFP) density (i) SFP 0.42 ($\rho = 0.42$ g/cm^3) (ii) SFP 0.49 ($\rho = 0.49$ g/cm^3) (iii) SFP 0.70 ($\rho = 0.70$ g/cm^3)	Increasing SFP density results in a decrease in nodal velocities and accelerations

Table 9: Summary of different parameters and respective effects on stiffened and curved panels under blast and impact loads.

Author (s)	Analysis method	Parameter lists	Remark
Furqan et al. [23]	FEA (LS-DYNA)	Unstiffened (U) flat panel charge masses (i) U 0.08925 kg (ii) U 0.1785 kg (iii) U 0.26675 kg (iv) U 0.08925 kg	While reducing charge mass by half, increase in standoff distance maximizes nodal displacement by double
		Unstiffened (U) flat panel standoff distances (i) U 10 (ii) U 15 (iii) U 20	Decrease in standoff distance significantly increases displacement and velocity values
Furqan et al. [23]	FEA (LS-DYNA)	Flat plate with stiffener configuration (i) No stiffener (ii) Single stiffener (iii) Double stiffener	Stiffeners with double layout placed under each side of the panel reveal a significant drop in acceleration values
		Plate configuration (i) Flat (ii) Convex (iii) Concave	The concave plate configuration exhibits an enormous decrease in peak displacement values

Table 10: Summary of different parameters and respective effects on mass concrete target and concrete blocks under combined blast and fragment impact loads.

Author (s)	Analysis method	Parameter lists	Remark
Yang et al. [4]	FEA (AUTODYN) and experimental	Concrete strength (i) Normal-strength (ii) High-strength	Damage and penetration depth for normal-strength concrete was large

Table 10: Continued.

Author (s)	Analysis method	Parameter lists	Remark
Leppanen et al. [27]	FEA (AUTODYN) and experimental	Load case (i) Only-fragment (ii) Blast-fragment	Large penetration and damage were obtained for combined load case
		Boundary condition (i) Free BC (ii) Fixed BC	Stress wave in free and fixed BC showed tensile and compressive wave, respectively

Table 11: Summary on FEA numerical simulation failure modes for mass concrete under combined explosion and penetrations projectile loads.

Damage propagations of different strength of mass concrete accompanied with penetration-explosion load case [4]

Normal strength concrete

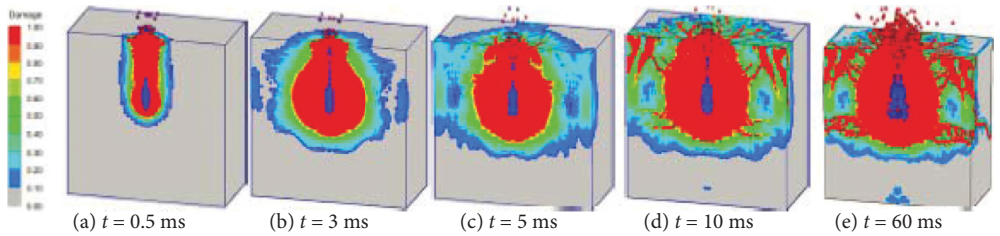

(a) $t = 0.5$ ms (b) $t = 3$ ms (c) $t = 5$ ms (d) $t = 10$ ms (e) $t = 60$ ms

High strength concrete

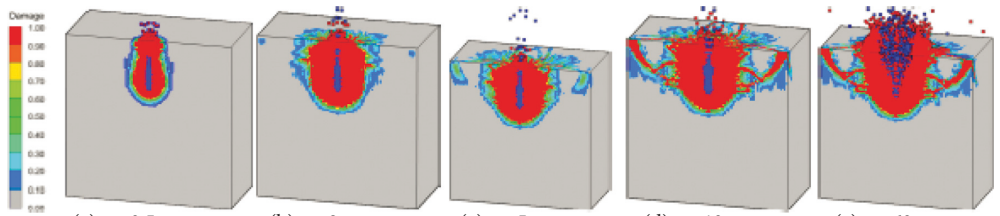

(a) $t = 0.5$ ms (b) $t = 3$ ms (c) $t = 5$ ms (d) $t = 10$ ms (e) $t = 60$ ms

Damage profile for concrete block subjected to simultaneous blast induced shock wave and fragment impact load with different boundary conditions [27]: (a) free and (b) fixed boundary conditions

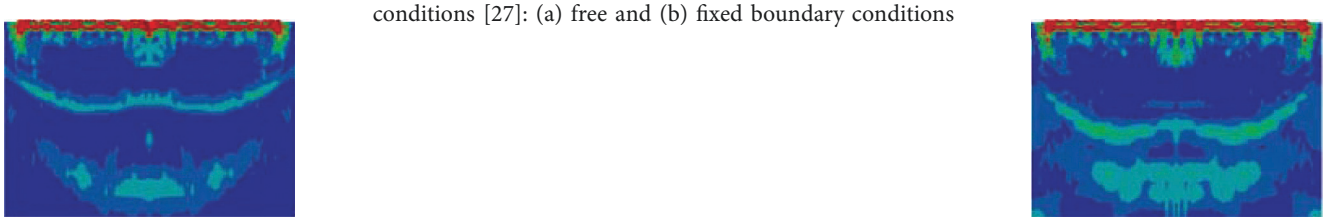

(a) (b)

use of holes at longitudinal bulkheads should rather be aligned in transverse direction.

The dynamic response of a stainless-steel plate when subjected to combined blast and sand impact loading was experimentally and numerically evaluated by Børvik et al. [25]. The authors deployed a fully coupled discrete particle finite element method of analysis to study and to capture physical interactions between explosive material and sand particles (dry and saturated sand). The authors inferred that explosive products with wet sand material revealed larger displacement values for different scaled distances.

Some studies urge considering the synergetic effects of combined blast and fragment impact loads on mass concrete. Lu et al. [26] experimentally examined damage

Table 12: Summary of experimentally tested damage on wall, panels, and concrete blocks subjected to combined blast and impact loads.

Discrete damage zones of front sides for different panels: (a) Concrete blocks and (b) aluminum foam sandwich

Linz et al. [16]

(a)

Santosa et al. [19]

(b)

Failure modes of concrete mass blocks prone to simultaneous loading of blast induced shock wave and fragment impact loads

Lu et al. [26]

Leppanen [27]

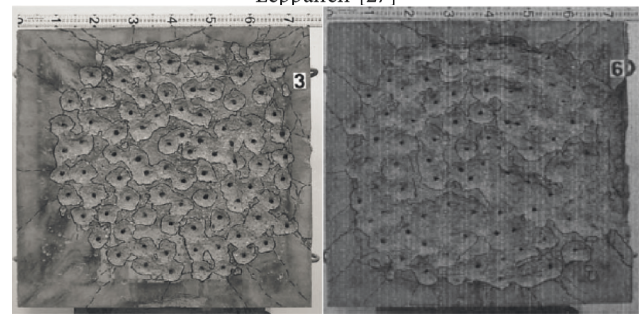

extents and failure modes of mass concrete when subjected to combined blast explosion and fragment penetration load cases. The researchers' novel work focuses on evaluation of penetration effects of projectiles, typically penetration speed and charge mass. The researchers designed coupled effect of explosion and fragment penetrations by clustering tests into two phases. The first stage encompasses a shot of a 30 mm caliber gun to a mass concrete target accompanied by a field based RDX explosion. From the experimental test results, it was observed that the damage properties and paths of mass concrete susceptible to combined effects of explosion and fragment penetration impact loads were complicated in nature. The researchers advocated that increasing impact coefficient of penetration of projectile mass (momentum) significantly affected by decreasing capacity of concrete mass. Besides, the authors articulated thickness of a concrete mass affects dynamic response of mass concrete.

Yang et al. [4] characterized damage modes of mass concrete target by simulating tip edge of concrete gravity dam when subjected to combined blast and impact loads. With the help of a nonlinear FEA packaged computational program (AUTODYN), the authors proposed three internal explosion models for the sake of computing effect of initial penetration processes and respective failures of a high-velocity projectile motion effects on damage modes of a specimen (mass concrete target). This was done by deploying advantages of symmetry accompanied by use of a spatial particles hydrodynamic-Lagrange based algorithm. The authors were able to assess damage performance of mass concrete with different concrete grade. Their results showed severe damage and less projectile impact load bearing capacity for mass concrete with normal strength concrete than high strength concrete. This implies that mass concrete strength has great influence on determination of damage modes and penetration depths and craters. The diagrammatic plots presented in Table 11 represent the extent of damage for a concrete with different strength classes (normal and high strength) under penetrating-explosion load scenario, on which the penetration was applied prior to explosion. As shown in Table 11, combined loads failure mechanism of high-strength concrete differs as compared to normal strength concrete.

Likewise, Leppanen [27] revealed an experimentally reported data on concrete block subjected to simultaneous combined action of blast and fragment impact loads. Further, Lagrangian-based numerical simulation was executed to evaluate dynamic response of concrete block under different standoff distances. The research work gives an insight to ways of tracing damage propagations of mass concrete under simultaneous combined blast and fragment impact loads under two different boundary conditions (BC), namely, free and fixed restraints. The numerical FEA was performed by using an explicit nonlinear computational program (AUTODYN) and during the simulation, use of symmetry allowed the researcher to use quarter size-scaled model. Forsake of simplification and ease of comparisons, two types of load cases were taken, namely, (a) only blast load and (b) combined blast and fragment impact loads. Table 12 exhibits a comparison of damage propagations in FEA models accompanied by aforementioned BCs. Their results show that large damage was obtained for combined load case compared to fragment-only load case.

5. Conclusions

In this paper, a state-of-the art review on structures under synergetic combined effects of blast and impact loads is presented. Literature reviews on design guidelines for analysis and design of structures under accidental loads are discussed and thoroughly reviewed in accordance with respective key features. Mass concrete blocks and various structural components including beams, columns, slabs, panels, and walls subjected to blast induced shock waves and fragment impact loads are also exclusively reviewed based on referring extended literature databases. The nature of loading mechanisms for simultaneous combined loading cases, dynamic response of the aforementioned structures, and ways of respective damage mitigation techniques are also discussed. The review considers two types of combined loading sequences, namely, blast-impact and impact-blast load cases.

This study implies neither current design guideline manuals (code of practices) nor designers account synergetic effects of combined blast and impact loads. Moreover, this paper shows presence of extensive experimental |data on structures prone to only-blast and only-impact loading whereas very few experimental investigations were available on structures susceptible to synergetic combined effects of blast and impact loads. The experimentally reported data were found to be scarcest in cases of beams and columns members. Due to this reason, currently, most researchers were forced to validate numerical models independently from previous only-impact and only-blast load experiments.

FE numerical models were efficient in capturing step-by-step progress of dynamic analyses and failure modes. Also, FEA results showed that impact-blast load case on which impact load was applied prior to blast induced shock waves aggravated damage was observed as compared to blast-impact load cases. Particularly, global failures were severely dependent on applied load sequence, i.e., when blast induced shock wave was detonated at time of initial peak impact force. On the contrary, for a load case when explosive and impactor were very close to a specimen (near-field effect), failure modes were not dependent on sequence of applied loads. In addition to this, the majority of researchers urged the community to study the effects of parameters such as loading locations, time lags, presence of axial loads, scaled distances, striking properties like size of impactor, and striking velocity. Those parameters affect dynamic response and damage modes of structures under combined blast and impact loads.

Finally, it is worthy to note there is a need to study synergetic effects of combined blast and impact loads at structural member level i.e., beams and columns, and the entire assembled global structural behavior through experimental investigations and high-end FEA.

Moreover, development and application of fragility models for framed structures under combined blast-impact loading cases are also required to be investigated as future research work to get deep insight into the behavior of framed structures under combined blast and impact loading.

Data Availability

All data are included in the manuscript

Conflicts of Interest

The authors declare that they have no conflicts of interest.

References

[1] Dod Ufc 3-340-02, *Unified Facilities Criteria; Structures to Resist the Effects of Accidental Explosions*, United States of America Department of America, USA, 2008.

[2] P. S. Bulson in *Proceedings of the Structures under shock and impact II: Proceedings to the Second International Conference*, Thomas Telford Services Ltd, Portsmouth, UK, 16 June 1992.

[3] U. Nyström and K. Gylltoft, "Numerical studies of the combined effects of blast and fragment loading," *International Journal of Impact Engineering*, vol. 36, no. 8, pp. 995–1005, 2009.

[4] G. Yang, G. Wang, W. Lu, P. Yan, and M. Chen, "Combined effects of penetration and explosion on damage characteristics of a mass concrete target," *Journal of Vibroengineering*, vol. 20, no. 4, pp. 1632–1651, 2018.

[5] J. M. Magallanes, R. Martinez, and J. W. Koening, *Experimental Results of the AISC Full-Scale Column Blast Test*, Chicago, 2006.

[6] G. Gholipour, C. Zhang, and M. Asma Alsadat, "Nonlinear failure analysis of bridge pier subjected to vessel impact combined with blast loads," *Ocean Engineering*, vol. 234, 2021.

[7] G. Gholipour, C. Zhang, and M. Asma Alsadat, "Numerical analysis of axially loaded RC columns subjected to the combination of impact and blast loads," *Engineering Structures*, vol. 219, pp. 1–25, 2020.

[8] G. Gholipour, C. Zhang, and M. Asma Alsadat, "Loading rate effects on the responses of simply supported RC beams subjected to the combination of impact and blast loads," *Engineering Structures*, vol. 201, pp. 109837–109917, 2019.

[9] G. Gholipour, C. Zhang, and M. Asma Alsadat, "Effects of axial load on nonlinear response of RC columns subjected to lateral impact load: ship-pier collision," *Engineering Failure Analysis*, vol. 91, pp. 397–418, 2018.

[10] H.-G. Kwak and M.J. Lee, "Blast and impact analyses of RC beams considering bond-slip effect and loading history of consitute materials," *International Journal of Concrete Structures and Materials*, vol. 134, pp. 1–13, 2018.

[11] R. R. Krishnan and S. R. Nair, "Structural behaviour of long and short reinforced concrete columns subjected to combined impact and blast loading," *India Technical Research Organisation*, vol. 8, no. 6, pp. 176–180, 2021.

[12] Z. Li and Y. Shi, "Methods for progressive collapse analysis of building structures under blast and impact loads," *Transactions of Tianjin University*, vol. 14, no. 5, pp. 329–339, 2008.

[13] R. Tao, R. Gao, Y. Li, Z. Chen, X. Ren, and D. Fang, "Experimental and numerical study on damage model of RC slabs under combined blast and fragment loading," *International Journal of Impact Engineering*, vol. 142, pp. 1–11, 2020.

[14] P. D., C. K. L. Linz and S. C. Fan, "Modelling of combined impact and blast loading on reinforced concrete slabs," *Latin America of Solids and Structures*, vol. 13, pp. 2266–2282, 2016.

[15] Y. J. M. Spencer and K. K. Wei, "Combined blast and fragment loading effects on reinforced concrete structures," *Engieering Structures*, vol. 248, pp. 1–16.

[16] P. D. Linz, T. Ching Fung, C. K. Lee, and W. Riedel, "Response mechanisms of reinforced concrete panels to the combined effects of close-in blast and fragments: an integrated experimental and numerical analysis," *International Journal of Protective Structures*, pp. 1–24, 2020.

[17] H. Y. Grisaro and A. N. Dancygier, "Dynamic response of RC elements subjected to combined loading blast and fragments," *Journal of Structural Engineering*, pp. 1–16, 2020.

[18] J. Ekström, *Concrete Structures Subjected to Blast Loading: Fracture Due to Dynamic Response*, MSc thesis. Göteborg, Sweden, 2015.

[19] S. P. Santosa, A. N. Pratomo, L. Gunawan, D. Widagdo, and I. S. Putra, "Numerical study and experimental validation of blastworthy structures using aluminum foam sandwich subjected to fragmented 8 kg TNT blast loading," *International Journal of Impact Engineering*, vol. 146, pp. 1–17, 2020.

[20] L. Li, Q. C. Zhang, R. Zhang et al., "A laboratory experimental technique for simulating combined blast and impact loading," *International Journal of Impact Engineering*, vol. 134, pp. 103382–103443, 2019.

[21] H. Y. Grisaro and A. N. Dancygier, "Characteristics of combined blast and fragments loading," *International Journal of Impact Engineering*, vol. 116, pp. 51–64, 2018.

[22] S. P. Santosa, F. Arifurrahman, M. H. Izzudin, D. Widagdo, and L. Gunawan, "Response analysis of blast impact loading of metal-foam sandwich panels," *Procedia Engineering*, vol. 173, pp. 495–502, 2017.

[23] A. Furqan, S. P. Santosa, A. S. Putra, D. Widagdo, L. Gunawan, and F. Arifurrahman, "Blast impact analysis of stiffened and curved panel structures," *Procedia Engineering*, vol. 173pp. 487–494, Indonesia, 2017.

[24] X.-shao Kong, W.-guo Wu, J. Li, P. Chen, and F. Liu, "Experimental and numerical investigation on a multi-layer protective structure under the synergistic effect of blast and fragment loadings," *International Journal of Impact Engineering*, vol. 65, pp. 146–162, 2014.

[25] T. Børvik, L. Olovsson, A. Hanssen, K. Dharmasena, H. Hansson, and H. Wadley, "A discrete particle approach to simulate the combined effect of blast and sand impact loading of steel plates," *Journal of the Mechanics and Physics of Solids*, vol. 59, no. 5, pp. 940–958, 2011.

[26] H. Lu, H. Geng, S. Sun, S. Yue, C. Song, and S. Feng, "Experimental study and damage effect analysis of concrete structures under the combined loadings of penetration and explosion," *Shock and Vibration*, vol. 2020, pp. 1–10, Article ID 2137945, 2020.

[27] J. Leppänen, "Experiments and numerical analyses of blast and fragment impacts on concrete," *International Journal of Impact Engineering*, vol. 31, no. 7, pp. 843–860, 2005.

[28] Asce, *Minimum Design Loads for Buildings and Other Structures*, American Society of Civil Engineers, USA, Second Edition, 2003.

[29] Asce, "Design of blast-resistant buildings in petrochemical facilities," *Task Committee on Blast-Resistant Design of the*

Petrochemical Committee of the Energy, Division of the American Society of Civil Engineers, Virginia, Second edition, 2010.

[30] Csa, *Design and Assessment of Buildings Subjected to Blast Loads CSA S850-12, Mississauga*, CSA Group, Ontario, Canada, 2012.

[31] Nafec, *Blast Resistant Structures: Design Manual 2.08*, Naval Facilities Engineering Command, Alexandria, Virginia, 1986.

[32] Doe, *A Manual for the Prediction of Blast and Fragment Loadings on Structures*, U. S. Department of Energy, Texas, 1980.

[33] Aashto, *Guide Specification and Commentary for Vessel Collision Design of Highway Bridges*, American Association of State Highway and Transportation Officials, Washington, 2nd edition, 2009.

[34] Cen Bs En 1991-1-1, *Actions on Structures. Part 1-7: General Actions Accidental Actions*, European Committee for Standardization, Brussels, Belgium, 2003.

[35] Uk's-Highway-Agency, "The design of highway bridges for vehicle collision loads," *Volume 1-Highway Structures: Approval Procedures and General Design; Section 3 General Design, Part 5-BD60/04*, Department of Transport, UK, 2004.

[36] Fema Fema 426, *Refernce Manual to Mitigate Potential Terrorist Attacks against Buildings; Providing protection to People and Buildings*, U.S Department of Homeland Security, USA, 2003.

[37] P. O. K. Krehl, *History of Shock Waves, Explosions, and Impact: A Chronological and Biographical Reference*, le-tex publishing service, Berlin Heidelberg, 2009.

[38] T. D. Ngo, P. Mendis, and A. Gupta, "Blast loading and blast effects on structures-An overview," *Journal of Structural Engineering*, vol. 199, pp. 76–91, 2007.

[39] Ceb, "Concrete structures under impact and impulsive loading," Synthesis Report, Comité Euro-International du Béton, Dubrovnik, 1988.

[40] M. Paz, *Structural Dynamics: Theory and Computation*, Van Nostrand Reinhold Company, New York, Second edition, 1985.

[41] g Hao, "Predictions of structural response to dynamic loads of different loading rates," *International Journal of Protective Structures-*, vol. 6, no. 4, pp. 585–605, 2015.

[42] S. Abebe and A. M. Tesfaye, "Performance assessment of reinforced concrete frame under close-in blast loading," *Advances in Civil Engineering*, vol. 2022, no. 1, 24 pages, Article ID 3979195, 2022.

[43] D. Rajkumar, R. Senthil, B. Bala Murali Kumar, K. AkshayaGomathi, and S. Mahesh Velan, "Numerical study on parametric analysis of reinforced concrete column under blast loading," *Journal of Performance of Constructed Facilities*, vol. 34, pp. 04019102–04019112, 2020.

[44] A. Dua, A. Braimah, and M. Kumar, "Experimental and numerical investigation of rectangular reinforced concrete columns under contact explosion effects," *Engineering Structures*, vol. 205, pp. 109891–109919, 2020.

[45] S.-E. Kim and D.-K. Thai, "Numerical invesitgation of the damage of RC members of RC members subjected to blast loading," *Engineering Failure Analysis*, vol. 92, pp. 350–367, 2018.

[46] A. Braimah and K. Conrad, "Effects of transverse reinforcement spacing on the response of reinforced concrete columns subjected to blast loading," *Engineering Structures*, vol. 142, pp. 148–164, 2017.

[47] T. Krauthammer, S. Astarlioglu, D. Morency, and T. P. Tran, "Behaviour of reinforced concrete columns under combined effects of axial and blast-induced transverse loads," *Engineering Structures*, vol. 55, pp. 26–34, 2013.

[48] Al-Thairy and Haitham, "Behaviour and failure of steel columns subjected to blast loads: numerical study and analytical approach," *Advances in Materials Science and Engineering*, vol. 2018, pp. 1–20, 2018.

[49] A. A. Nassr, A. G. Razaqpur, M. J. Tait, M. Campidelli, and S. Foo, "Dynamic response of steel columns subjected to blast loading," *Journal of Structural Engineering*, vol. 140, no. 7, pp. 04014036–4014115, 2014.

[50] R. L. Shope, "Response of wide flange steel columns subjected to constant axial loads and lateral blast load," PhD dissertation, Blacksburg, Virginia, 2006.

[51] T. Krauthammer, "AISC research on structural structural steel to resist blast and progressive collapse," *AISC Steel Building Symposium: Blast and Progressive Collapase Resistance*, vol. December, pp. 4-5, 2003.

[52] A. Dua, A. Braimah, and M. Kumar, "Contact explosion response of reinforced concrete columns: experimental and validation of numerical model," *Building Tomorrow Society*, vol. 173, pp. 1–10, 2018.

[53] F. Siba, "Near-field explosion effects on reinforced concrete columns: an experimental investigation," Theses, Dissertations, Ottawa, Ontario, 2014.

[54] B. Li, A. Nair, and Q. Kai, "Residual axial capacity of reinforced concrete columns with simulated blast damage," *Journal of Performance of Constructed Facilities*, vol. 26, no. 3, pp. 287–299, 2012.

[55] T.-shuan Zhuang, M.-yang Wang, J. Wu, C.-yu Yang, T. Zhang, and C. Gao, "Experimental investigation on dynamic response and damage models of circular RC columns subjected to underwater explosions," *Defence Technology*, vol. 16, no. 4, pp. 856–875, 2020.

[56] G. Wang, W. Lu, G. Yang, X. Zhao, Y. Peng, and M. Chen, "Cross-section effects on anti-knock performance of RC columns subjected to air and underwater explosions," *Ocean Engineering*, vol. 181, pp. 252–266, 2019.

[57] Y. Liu, J.-bo Yan, and F.-lei Huang, "Behavior of reinforced concrete beams and columns subjected to blast loading," *Defence Technology*, vol. 14, no. 5, pp. 550–559, 2018.

[58] S. Andersson and H. Karlsson, "Structural response of reinforced concrete beams subjected to explosions," MSc Thesis, Göteborg, Sweden, 2012.

[59] G. Carta and F. Stochino, "Theoretical models to predict the flexural failure of reinforced concrete beams under blast loads," *Engineering Structures*, vol. 49, pp. 306–315, 2013.

[60] Q. Fang, Q.-H. Qian, and Y.-L. Shi, "A rate-sensitive analysis of RC beams subjected to blast loads," *Transactions on the Built Environment*, vol. 22, pp. 221–230, 1996.

[61] Li Chen, B. Rao, F. Qin, J. Hong, Z.-xian Liu, and H.-bo Xiang, "Dynamic response of reinforced concrete beams under double-end-initiated close-in explosion," *Defence Technology*, vol. 14, pp. 527–539, 2018.

[62] D. Zhang, S.J. Yao, F. Lu et al., "Experimental study on scaling of RC beams under close-in blast loading," *Engineering Failure Analysis*, vol. 33, pp. 497–504, 2013.

[63] W. Zhang, X. Kong, Y. Qu, and Q. Zhao, "Numerical simulation of cracked reinforced concrete slabs subjected to blast loading," *Civil Engineering Journal*, vol. 4, no. 2, pp. 320–333, 2018.

[64] N. K. Vijitha, B. P. Ammu, and R. Ahani, "Prediction of blast loading and its effects on waffle slab," *International Journal*

for Research in Applied Science and Engineering Technology, vol. 5, no. V, pp. 864–871, 2017.

[65] F. Omidinasab, H. Rezaei, P. Beiranv, and M. H. Naserifard, "Effects of the blast load on FRP panels and analysis of resistance," *Indian journals of science and technology*, vol. 9, no. 18, pp. 1–9, 2016.

[66] N. Anandavalli, N. Lakshmanan, J. Rajasankar, and A. Prakash, "Numerical studies on blast loaded steel-concrete composite panels," *JCES*, vol. 1, no. 3, pp. 102–108, 2012.

[67] Nalagotla and J. K. Reddy, *Pressure-impulse Diagrams Using Finite Element Analysis for Reinforced concrete Slabs Subjected to Blast Loading*, Mo Space, USA, 2013.

[68] C. Wu, J. Jones, D. J. Oechlers et al., "Finite difference analysis of simply supported RC slabs for blast loading," *Engineering Structures*, vol. 31, pp. 2825–2832, 2009.

[69] A. Khadid, N. Lahbari, and A. Fourar, "Blast loaded stiffened plates," *Journal of Engineering and Applied Sciences*, vol. 2, no. 2, pp. 456–461, 2007.

[70] J. Fan, "Response of reinforced concrete reservior walls subjected to blast loading," MSc Thesis, Ottawa, 2014.

[71] N. T. Rouse, "The mitigation effects of a barrier wall on blast wave pressures," MSc Thesis, USA, 2010.

[72] K. Wheaton, "Blast assessment of load bearing reinforced concrete shear walls," MSc Thesis, Pennsylvania, 2005.

[73] S. D. Adhikary, K. Patel, and A. Goswami, "Response characterization of highway bridge piers subjected to blast loading," *Structural Concrete*, vol. 21, no. 6, pp. 2377–2395, 2020.

[74] D. H. T. Priyawakode and G. R. Gandhe, "Blast load analysis on bridge subjected to various standoff distance," *International Journal of Engineering Research*, vol. V9, no. 07, pp. 935–938, 2020.

[75] Y. Li and S. He, "Research of steel-concrete composite bridge under blasting loads," *Advances in Civil Engineering*, vol. 2018, pp. 1–9, Article ID 5748278, 2018.

[76] Lu Liu, Z. Zong, B. Tang, and M. Li, "Damage assessment of an RC pier under noncontact blast loading based on P-I curves," *Shock and Vibration*, vol. 2018, pp. 1–12, Article ID 9204036, 2018.

[77] Z. Zong, S. Yuan, H. Hong, and J. Li, "A study of RC bridge columns under contact explosion," *International Journal of Impact Engineering*, vol. 109, pp. 378–390, 2017.

[78] Y. Pan, C. E. Ventura, and M. M. S. Cheung, "Performance of highway bridges subjected to blast loads," *Engineering Structures*, vol. 151, pp. 788–801, 2017.

[79] D. Makovicka and D. MakovickaJr., "Dynamic response of structures under blast load," *Journal of Civil Engineering and Architecture*, vol. 10, pp. 421–429, 2016.

[80] R.-B. Deng and X.-L. Jin, "Numerical simulation of bridge damage under blast loads," *WSEAS Transactions on Computers*, vol. 8, no. 9, pp. 1564–1574, 2009.

[81] F. A. Abdelahad, "Analysis of blast/explosion resistant reinforced concrete solid slab and T-beam bridges," MSc Thesis, Florida; USA, 2008.

[82] S. Fujikura, M. Bruneau, and D. Lopez-Garcia, "Experimental investigation of multihazard resistant bridge piers having concrete-filled steel tube under blast loading," *Journal of Bridge Engineering*, vol. 13, no. 6, pp. 586–594, 2008.

[83] K. A. Marchand, D. G. Winget, and E. B. Williamson, "Analysis and design of critical bridges subjected to blast loads," *Journal of Structural Engineering*, vol. 131, no. 8, pp. 1243–1255, 2005.

[84] K. Marchand, D. G. Winget, and E. B. Williamson, "Analysis of blast loads on bridge substructures," *Structures Under Shock and Impact*, vol. VIII, pp. 151–160, 2004.

[85] E. Brunesi and F. Parisi, "Progressive collapse fragility of European reinforced concrete buildings," in *Proceedings of the 13th International Conference on Applications of Statistics and Probability in Civil Engineering ICASP13*, pp. 1–8, CityU Scholars, Republic of Korea, 26 May 2019.

[86] E. Brunesi, R. Nascimbene, and F. Parisi, "Progressive collapse fragility models of RC framed buildings based on pushdown analysis," in *Proceedings of the VII European Congress on Computational Methods in Applied Sciences and Engineering*, Crete Island, 13 October 2016.

[87] E. Brunesi, R. Nascimbene, F. Parisi, and N. Augenti, "Progressive collapse fragility of reinforced concrete framed structures through incremental dynamic analysis," *Engineering Structures*, vol. 104, pp. 65–79, 2015.

[88] A. Kumar and V. Matsagar, "Blast fragility and sensitivity analyses of steel moment frames with plan irregularities," *International Journal of Steel Structures*, vol. 18, no. 5, pp. 1684–1698, 2018.

[89] Y. Ding, X. Song, and H.-T. Zhu, "Probabilistic progressive collapse analysis of steel frame structures against blast loads," *Engineering Structures*, vol. 147, 2017.

[90] J.-L. Le and B. Xue, "Stochasstic computational model for progressive collapse of reinforced concrete buildings," *Journal of Structural Engineering*, vol. 142, pp. 1–14, 2016.

[91] J.-L. Le and B. Xue, "Probabilistic analysis of reinforced concrete frame structures against progressive collapse," *Engineering Structures*, vol. 76, pp. 313–323, 2014.

[92] G. Appuhamilage, "Effects of blast loading on reinforced concrete facade systems," PhD Dissertation, Melbourne, Australia, 2015.

[93] F. L. Mendoza and M. A. Josef, "Concrete beams subjected to drop-weight impact and static load," MSc Thesis, Gothenburg, Sweden, 2017.

[94] Y. Qasrawi, P. J. Heffernan, and A. Fam, "Numerical modelling of concrete-filled FRP tubes dynamic behaviour under blast and impact loading," *Journal of Structural Engineering*, pp. 1–13, 2015.

[95] T. A. Mohammed and T. Alebachew, "Numerical investigation of as-built and carbon fiber reinforced polymer retrofitted reinforced concrete beam with web openings under impact loading," *ASEAN Engineering Journal*, vol. 12, no. 1, pp. 173–182, 2022.

[96] Y. C. Wang and H. Al-Thairy, "A numerical study of the behaviour and failure modes of axially compressed steel columns subjected to transverse impact," *International Journal of Impact Engineering*, vol. 38, no. 8-9, pp. 732–744, 2011.

[97] S. Saatci and F. J. Vecchio, "Nonlinear finite element modelling of reinforced concrete structures under impact loads," *ACI Structural Journal*, pp. 717–725, 2009.

[98] Sangi and Abdul Jabbar, "Reinforced concrete structures under impact loads," PhD Dissertation, Scotland, 2011.

[99] T. A. Mohammed and A. Parvin, "Evaluating damage scale model of concrete materials using test data," *Advances in concrete construction*, vol. 1, no. 4, pp. 289–304, 2013.

[100] J. C. Xiao, J. F. Liu, C. Bai, J. Y. Mao, and K. J. Ma, "Dynamic behavior of composite beams under imapct load," *Key Engineering Materials*, vol. 400-402, pp. 783–787, 2009.

[101] P. Pintado and J. Morton, "On the scaling of impact loaded composite beams," *Composite Structures*, vol. 27, no. 4, pp. 357–365, 1994.

[102] Ö. Anil, T. Yilmaz, and N. Kiraç, "Experimental investigation of axial loaded reinforced concrete square column subjected to lateral low-velocity impact loading," *International Federation for Structural Concrete*, vol. 20, pp. 1–21, 2019.

[103] W. Fan, B. Liu, and W. Guo, "Experimental investigation and improved FE modelling of axially-loaded circular RC columns under lateral impact loading," *Engineering Structures*, vol. 152, pp. 619–642, 2017.

[104] Z. Weiyi and Q. Guo, "Displacement response analysis of steel-concrete composite panels subjected to impact loadings," *International Journal of Impact Engineering*, vol. 131, pp. 272–281, 2019.

[105] S. D. Adhikary, A. Goswami, and B. Li, "Predicting the punching shear failure of concrete slabs under low velocity impact loading," *Engineering Structures*, vol. 184, pp. 37–51, 2019.

[106] S. Ur Rehman, "Finite element analysis of impact-perforated reinforced concrete slabs," MSc Thesis, Espoo, Finland, 2017.

[107] R. T. Erdem and E. Gücüyen, "Non-linear analysis of reinforced concrete slabs under impact effect," *Građevinar*, vol. 69, pp. 479–487, 2017.

[108] J. Sagaseta, K. Micallef, M. Fernandez Ruiz, and A. Muttoni, "Assessing punching shear failure in reinforced concrete flat slabs subjected to localised impact loading," *International Journal of Impact Engineering*, vol. 71, pp. 17–33, 2014.

[109] F. Kassem, "Reliability of reinforced concrete structures: case of slabs subjected to impact," PhD Dissertation, Lyon, November, 2015.

[110] Ö. Anil, T. Yilmaz, N. Kiraç, R. T. Erdem, R. Tugrul Erdem, and C. Sezer, "Low-velocity impact behaviour of two way RC slab strengthening with CFRP strips," *Construction and Building Materials*, vol. 186, pp. 1046–1063, 2018.

[111] H. Othman and H. Marzouk, "An experimental investigation on the effect of steel reinforcement on impact response of reinforced concrete plates," *International Journal of Impact Engineering*, vol. 88, pp. 12–21, 2016.

[112] P. Isaac, A. Darby, Tim Ibell, and M. Evernden, "Experimental investigation into the force propagation velocity due to hard impacts on reinforced concrete memebers," *International Journal of Impact Engineering*, vol. 100, pp. 1–25, 2016.

[113] S. D. Adhikary, B. Li, and K. Fujikake, "Low velocity impact response of reinforced concrete beams: experimental and numerical investigation," *International Journal of Protective Structures*-, vol. 6, no. 1, pp. 81–111, 2015.

[114] A. Andersson, "Impact loading on concrete slabs: experimental tests and numerical simullations," MSc Thesis, Stockholm, Sweden, 2014.

[115] T. D. Hrynyk and F. J. Vecchio, "Behavior of steel fibre-reinforced concrete slabs under impact load," *ACI Structural Journal*, pp. 1213–1223, 2014.

[116] B. Batarlar, "Behavior of reinforced concrete slabs subjected to impact loads," MSc Thesis, İzmir, 2013.

[117] N. Kishi, H. Mikami, and T. Ando, "Impact-resistant behaviour of shear-failure-type RC beams under falling-weight impact loading," *Structures Under Shock and Impact*, vol. VII, pp. 500–508, 2002.

[118] J. Leppänen, "Concrete subjected to projectile and fragment impacts: modelling of crack softening and strain rate dependency in tension," *International Journal of Impact Engineering*, vol. 32, no. 11, pp. 1828–1841, 2006.

[119] J. Leppänen, *Concrete Structures Subjected to Fragment Impacts*, Götenborg, Sweden, 2004.

[120] A. Tesfaye and A. Parvin, "Vehicle collision impact response of bridge pier strengthened with composites," *Practice Periodical on Structural Design and Construction*, pp. 1–9, 2020.

[121] G. Gholipour, C. Zhang, and M. Li, "Effects of soil-pile interaction on the response of bridge pier to barge collision using energy distribution method," *Structure and Infrastructure Engineering*, vol. 14, no. 11, pp. 1520–1534, 2018.

[122] H. Hao, T. V. Do, and T. M. Pham, "Dynamic response and failure modes of bridge columns under vehicle collision," *Engineering Structures*, vol. 156, pp. 243–259, 2018.

[123] W. Fan, X. Xu, Z. Zhang, and X. Shao, "Performance and sensitivity analysis of UHPFRC-strengthened bridge columns subjected to vehicle collisions," *Engineering Structures*, vol. 173, pp. 251–268, 2018.

[124] H. Jiang, J. Wang, Mi G. Chorzepa, and J. Zhao, "Numerical investigation of progressive collapse of a multispan continous bridge subjected to vessel collision," *Journal of Bridge Engineering*, vol. 22, pp. 1–16, 2017.

[125] Y. Sha and H. Hao, "Nonlinear finite element analysis of barge collision with a single bridge pier," *Engineering Structures*, vol. 41, pp. 63–76, 2012.